

Development of chemiresistive sensors made of carbon nanotubes to detect *E. coli*

M.A.Sc. Thesis – Arash Fattahi; McMaster University –Materials Science and  
Engineering

Development of chemiresistive sensors made of carbon nanotubes to detect *E. coli*

By Arash Fattahi, B.Sc., M.A.Sc.

A Thesis Submitted to the School of Graduate Studies in Partial Fulfilment of the  
Requirements for the Degree Master of Applied Science

McMaster University © Copyright by Arash Fattahi, June 2019

M.A.Sc. Thesis – Arash Fattahi; McMaster University –Materials Science and Engineering

McMaster University Master of Applied Science (2019) Hamilton Ontario (Materials Science and Engineering)

TITLE: Development of chemiresistive sensors made of carbon nanotubes to detect *E. coli*  
AUTHOR: Arash Fattahi, B.Sc. (Isfahan University of Technology, Iran), SUPERVISOR: Professor I. K. Puri NUMBER OF PAGES: xxiv, 64.

## ABSTRACT

Rapid detection of bacteria is crucial to control the increasing number of outbreaks and food recalls. The current detection method relies on a lab based bacterial culture that takes several hours to few days to test the samples. Here, we demonstrate a facile and rapid fabrication of a chemiresistive sensor using multiwalled carbon nanotubes (MWCNTs) for detecting *E. coli* bacteria. MWCNTs functionalized with magnetic nanoparticles, act as the transduction element and magnetically assisted printing is used to obtain a thin conducting strip. The sensing strip is functionalized with specific antibodies for target bacteria. *E. coli* K12 is chosen as the target bacteria and *Bacillus subtilis* as the negative control. Specific binding between antibody and bacteria is investigated by measuring the change in the resistance of the strip. The change in resistance is proportional to the increasing concentration of bacteria present in the sample. A response time of ~ 2 minutes can be attributed to the sensor. The detection limit with whole cell is in the range of  $10^5$  cells/ml, whereas with the cell lysates, the limit of detection improves to  $10^3$  cells/ml.

## Table of content

1. Introduction.....	1
1.1 Biosensors .....	1
1.2 Electrochemical biosensor.....	5
1.3 <i>Escherichia coli</i> Biosensors .....	8
2. Carbon nanotubes: properties and use in biosensors .....	11
2.1 Introduction .....	11
2.2 Carbon Nanomaterials for Biosensing .....	11
2.2.1 Structures and types of CNTs.....	13
2.2.2 Properties of CNTs .....	15
2.2.3 Application of CNTs.....	16
2.2.4 Synthesis method.....	17
2.2.5 Challenges in handling CNTs.....	18
2.3 Functionalization of CNTs Biosensors .....	19
2.4 Magnetized CNTs-based sensors .....	20
2.4.1 Classification of Magnetic Materials.....	20
2.4.2 Magnetic domains.....	22
2.4.3 Magnetism in small dimensions .....	23
2.4.2 Magnetic Nanomaterials.....	24
2.5 Magnetization of Carbon Nanotubes.....	24
2.6 mCNTs Biosensor: Background.....	25
2.6.1 Sensing mechanism of CNTs-based biosensor.....	26
2.6.1.1 Electrostatic gating.....	27
2.6.1.2 Chemical doping .....	28
3. Developing a biosensor printed strip out of MWCNTs .....	30
3.1 Introduction .....	30
3.2 Methodology .....	30
3.2.1 Materials and Reagents.....	30
3.2.2 Synthesis of magnetized carbon nanotubes (mCNTs).....	31
3.2.3 Bio-ink fabrication.....	32
3.2.4 Printing the bio-ink on the substrate.....	33

3.2.5	Flow cell design .....	34
3.2.6	Functionalizing the strips with Abs .....	35
3.3	Results and Discussion .....	35
3.3.1	Optical and Electrical characterization of printed sensing strip .....	35
3.3.3	Fluorescent microscopy imaging .....	37
3.4	Conclusion .....	39
4.	mCNTs based chemiresistive sensor for bacteria detection.....	40
4.1	Introduction .....	40
4.2	mCNTs based biosensor for detecting bacteria.....	40
4.3	Bacteria detection .....	43
4.3.1	Introduction to bacteria.....	43
4.3.2	Fabrication method .....	45
4.4	Results and discussions .....	45
4.4.1	Visualization of bacteria .....	45
4.4.2	E. coli K12 sensing .....	47
4.4.2.1	Detection of E. coli whole cell .....	48
4.4.2.1	Detection of E. coli with cell lysates .....	50
5.	Summary and Future Work.....	52
5.1	Conclusion.....	52
5.2	Future Work .....	52
5.3	Summary .....	53
6.	References .....	55

LIST OF FIGURES

Figure 2.1: Carbon structure exhibiting different hybridization states:  $sp^3$  hybridized diamond (left) and  $sp^2$  hybridized graphite (right).....12

Figure 2.2: Physical structure of CNTs a) yellow and green lines represent armchair and zigzag configuration respectively.  $C_h$  is the chiral vector defined by unit vectors  $a_1$  and  $a_2$  and angle  $\theta$ , b) chiral SWCNT- (7,2), c) armchair SWCNT- (7,7) and d) zigzag SWCNT (9,0).....15

Figure 2.3: Different types of magnetism: (a) Ferromagnetism, (b) Paramagnetism. (c) Anti-ferromagnetism, and (d) Ferrimagnetism.....22

Figure 2.4: The relation between the coercivity and the particle size.....24

Figure 3.1: Schematic of the steps involved in ink preparation and printing: a) magnetized carbon nanotubes with available carboxylic groups on the surface, b) addition of Tween20 to avoid agglomeration and c) magnetically assisted printing of the ink on a glass slide to form a thin conducting strip.....33

Figure 3.2: Functionalization of the bio-strip: (a) fabrication of flow cell over the sensing strip, (b) antibody immobilization and (c) specific binding of bacterial cells with the specific antibodies on mCNTs .....33

Figure 3.3: Characterization of the printed sensing strips: a) average width of printed strips measured with a microscope, b) average resistance of functionalized strips measured using multimeter .....35

Figure 3.4: Visualization of *E. coli* Abs. immobilized on the surface of mCNTs. Brightfield and fluorescent microscopy images of FITC labelled secondary antibody for different concentrations of (a) 50 $\mu$ g/ml, (b) 10 $\mu$ g/ml and (c) 1 $\mu$ g/ml. The fluorescence indicates the successful conjugation of FITC labelled antibody with the primary *E. coli* Abs covalently bonded to the surface of mCNTs. Panel (d) shows the effect of fluorescent Abs on the ink without any primary Ab....34

Figure 4.1:Optical microscopy images for different concentration of bacteria.....45

Figure 4.2. Performance of the biosensor with sample containing whole bacterial cell. (a) Average of the normalized current with time for different bacterial concentrations and (b) the normalized current response at  $t = 120s$  with standard deviations. Number of samples,  $n \geq 4$ .....49

Figure 4.3: Performance of the biosensor with sample containing whole bacterial cell. (a) Average of the normalized current with time for different bacterial concentrations and (b) the normalized current response at  $t = 120s$  with standard deviations. Number of samples,  $n \geq 4$  .....50

Figure 4.4: Performance of the biosensor with sample containing bacterial cell lysate. (a) The average variation of the normalized current with time for different bacterial concentrations and (b) the normalized current response at  $t = 120s$  with standard deviations. Number of samples,  $n \geq 4$ .....51

LIST OF TABLES

Table 4.1 Number of bacteria calculated in each concentration of bacteria by optical microscope versus optical density measurement..... 47



#### ACKNOWLEDGEMENTS:

I would like to acknowledge all people whom without their help and support this work could not be completed at all. I wish to offer my most heartfelt thanks to them.

First of all, I would like to thank my research supervisor, Professor Ishwar K. Puri, who has been the best support for me not only as an academic supervisor, but also as a great support in all different stages of my career during my master program. During my tenure, he contributed to a rewarding graduate school experience by giving me intellectual freedom in my work, engaging me in new ideas, and demanding a high quality of work in all my endeavors. Thank you for the advice, support, and willingness that allowed me to pursue research on topics for which I am truly passionate.

Also, I would like to thank Dr. Rakesh Prasad Sahu who not only greatly mentored me during my researches but also guided me with his precious advice and supports in my master program. Additionally, I am very grateful for the friendship of all of the Multiphysics Research Group, especially Dr. Srivatsa Aithal, Dr. Fei Geng, Tamaghna Gupta, Krishna Jangid, Sarah Mishriki, Mohammed Nawwar, Ri Chen, and Tahereh Majdi,, whom I worked closely and puzzled over many problems. They helped me in numerous ways during various stages of my master. Thanks to Sarah, Tamaghna, and Dr. Fei Geng whom opened my eyes to the beauty of biology and provided me with many biological knowledge.

I also deeply appreciate the research funding and support provided by the Natural Science Engineering Research Council of Canada (NSERC) for making this research possible.

Finally, and most importantly, I would like to acknowledge friends and family who supported me during my time here. I would like to thank my parents, for all of their endless sacrifices whom without them, I would not be able to take one single step in this path.

## LIST OF ABBREVIATIONS

Ab	Antibody
Ag	Antigen
aMWNT	Activated multiwalled carbon nanotubes
Bioink	Biological ink
BS	Bacillus Subtilis
BSA	Bovine serum albumin
CNT	Carbon nanotube
CVD	Chemical vapor deposition
$D_c$	Critical diameter
Dc	Direct current
DI Water	Deionized water
$D_s$	Super paramagnetic diameter
DW	Distilled Water
DWNT	Double walled carbon nanotubes
EDC/NHS	1-ethyl-3-(3-dimethylaminopropyl)/ N-Hydroxysuccinimide
ELISA	Enzyme linked immunosorbent assay
E. coli	Escherichia coli
FITC	Fluorescein isothiocyanate
LB	Luria Bertani
mBioink	Magnetic biological ink
mCNT	Magnetic carbon nanotube
MNP	Magnetic nanoparticle
MWNT	Multiwalled carbon nanotube
mMWNT	Magnetic multiwalled carbon nanotube
NP	Nanoparticle
PBS	Phosphate buffered saline
PCR	Polymeric chain reaction

SWNT            Single walled carbon nanotubes

LIST OF SYMBOLS

$c$	Chiral vector
$\theta$	Angle
$r$	Radius
$\chi$	Magnetic susceptibility
$\mu$	Permeability
$H$	Magnetic field
$E$	Electric field
$B$	Magnetic induction
$M$	Magnetization
$H_c$	Coercive field
$I$	Electric current
$J$	Electric current density
$q$	Electric charge
$A$	Area
$m$	Magnetic moment
$N_A$	Avogadro's Number
$T$	Temperature
$a, b, \text{ and } c$	Lattice space parameters
$\chi_B$	Boltzmann's constant
$\epsilon \tau$	permittivity in a vacuum
$e$	elementary charge
$I$	ionic strength

# 1. Introduction

## 1.1 Biosensors

Biosensor, a term that stands for “Biological Sensor”, is an analytical device that measures biological or chemical reactions by generating electrical signals proportional to the concentration of the analyte in the reaction [1]. A typical biosensor consists of the following components: (1) Analyte; a biological sample derived from human body, food and environment that needs to be detected. For example, lake water is an analyte to detect pathogens. The pathogens diffuse from the solution to the surface of the biosensor, reacts specifically and efficiently with the recognition elements. (2) Bioreceptor; a molecule that specifically recognises the analyte. Enzymes, antibodies and deoxyribonucleic acid (DNA) are some examples of bioreceptors. The process of signal generation (in the form of light, heat, pH, charge or mass change, etc.) upon interaction of bioreceptor with the analyte is termed bio-recognition. (3) Transducer; an element that converts biological response to a measurable output. Most transducers produce either optical or electrical signals and are usually proportional to the amount of analyte-bioreceptor interactions. (4) Electronics; the part of a signal processing system in a biosensor that amplifies and processes the transduced signal in an appropriate quantified format as an input for display system. (5) Display; consists of a user interpretation system such as the liquid crystal display of a computer or a direct printer that generates numbers or curves understandable by the user. This part often consists of a combination of hardware and software components that generates results of

the biosensor either in numeric, graphic, tabular or an image format, depending on the requirements of the end user [2].

Biosensors are employed in a wide range of applications from diagnosis of life-threatening diseases to detection of pollutants. They are becoming a crucial part of modern life due to fast response and detection at sub-nanomolar (nM) concentrations of specific biomolecules, such as proteins, DNA and specially pathogens. Being able to detect low concentrations of pathogens, helps rapid detection of harmful molecules in an environment. In this case, sensors can detect the species in a short period of time which leads to early control and decrease the lifetime for these species in environmental samples.

Every biosensor possesses several properties and optimisation of these properties is reflected on the performance of biosensor. The main features of biosensors are: selectivity, sensitivity, reproducibility, stability and linearity. Selectivity can be considered as the most important characteristics of a biosensor. It is the ability of a bioreceptor to detect a specific analyte within a sample containing other contaminations and admixtures. The best example of selectivity is perhaps the antigen-antibody binding. In general, antibodies act as bioreceptors and are immobilised on to the surface of the transducer. Antigen presents in a solution (usually buffer containing salts) is then exposed to the transducer where antibodies interact specifically with the target antigens. Sensitivity is the minimum amount of analyte that can be detected using a biosensor. It is also defined as limit of detection (LOD). In medical and environmental monitoring, a biosensor is required to detect analyte in sub-nanomolar concentration. For example, a prostate specific antigen (PSA) concentration of 4 ng/ml in blood is associated with prostate cancer for which doctors suggest biopsy tests.

Reproducibility which brings high reliability for the biosensor, is the ability to provide identical responses for multiple experiments performed under similar conditions. Two features of reproducibility in a biosensor is precision and accuracy of the transducer and electronics. Precision is the ability of the biosensor to generate same results each time a sample is measured and accuracy is providing a mean value close to the true value out of a biosensor when sample is measured several times. Stability is the degree of susceptibility to ambient disturbance in the vicinity of biosensor. These disturbances can cause a drift in the output signals of a biosensor under measurement. This can cause an error in the measured concentration and can affect the precision and accuracy of the biosensor. In the case of long incubation time or continuous monitoring for a biosensor, this is the most crucial feature. The response of transducers and electronics can be temperature-sensitive, which may influence the stability of a biosensor. Therefore, appropriate tuning of electronics is required to ensure a stable response of the sensor. Another factor that can influence the stability is the affinity of the bioreceptor, which is the degree to which the analyte binds to the bioreceptor. Bioreceptors with high affinities encourage either strong electrostatic bonding or covalent linkage of the analyte that fortifies the stability of a biosensor. Another factor that affects the stability of a measurement is the degradation of the bioreceptor over a period of time. Linearity is the relation between responses of measurements with different concentrations of analyte to a straight line. In other word, the ratio of output to concentration of analyte is a fixed value which is the sensitivity of the biosensors [3].



Consequently, rapid detection of molecules with good selectivity and high sensitivity is significantly important since diseases caused due to harmful pathogens such as *Escherichia coli* could be prevented. One of the existing methods used for detection of biomolecules include enzyme-linked immunosorbent assay (ELISA). This method requires long incubation times, complicated instrumentation, large sample volume and, also trained professionals [4]. The above-mentioned challenges in detection of biomolecules using the conventional techniques, has led to design and fabricate a real-time point of care pathogen detection device [5].

According to literature review, most biosensors used to detect biomolecules suffer from good sensitivity and specificity. Relevant techniques available nowadays are Whispering-gallery microlasers [6-8], microring resonators [9,10] silicon nanowire field effect transistors (FET) [11-13], polymer nanowires [14,15] and surface plasmon resonance (SPR) [16-18]. These techniques have high sensitivity but involve complicated instrumentation, sophisticated data analysis in combination with long procedures that has prevented the wide usage of these techniques to a great extent.

In the case of pathogen detection, traditional techniques are also not relevant because of complicated procedures [19]. The traditional methods in this field involves culturing and colony counting methods and polymerase chain reaction (PCR). Among these two techniques, culture and colony method is time extensive [19]. A label free biosensor, at low cost providing rapid detection of pathogen with no sophisticated facilities is the ultimate goal.

Biosensors have a wide range of applications including environmental monitoring, drug delivery, food industry, clinical applications and so on. Based on the applications, biosensors could be fabricated using different working principles. The main techniques used in biosensing are electrochemical, optical and physical. For example, electrochemical biosensing techniques are mainly used in clinical applications to detect cancer biomarkers [20-22]. Another way to classify biosensors is by considering the response time to different analytes. For example, in food industry, biosensor should have a fast response in order to avoid spreading of pathogens [3]. In this case, cost-effective and disposable biosensors are primarily used. On the other hand, environmental monitoring and especially pollutant screening is performed in few hours to several days. In both of these categories, application of biosensor is limited because of the complexities involved [20]. Among different techniques, electrochemical biosensors are of more interest due to fast response and cost-effective process.

## 1.2 Electrochemical biosensor

Optical sensing techniques nowadays are used extensively for medical applications [19]. In order to increase the sensitivity of these sensor, nanostructure materials are applied to the sensor. However, there are some disadvantages regarding these techniques such as sample preparation which is time consuming and the ability for performing expensive and non-portable high-tech devices, that make users choose other techniques. On the other hand, electrochemical sensors are using components which are less complicated, which are cheap as well, easy to use and being available for applying on sites which make them suitable for

label-free detection approaches. Development of silicon based ion sensitive field effect transistor (ISFET) by Bergveld in 1970 [24] decreased the time response and improved the sensitivity of electrical biosensors to a great extent. The limit of detection for first generation of ISFET reached to micromolar ( $\mu\text{M}$ ). Although this LOD can be useful for some types of analytes, such as glucose level in blood, there are many other biomolecules that requires lower limit of detection [25]. Lack of sensitivity has led to extensive research on one-dimensional nanomaterials based electrical biosensor over the past decade [26]. Due to high sensitivity and specificity, and also lab on chip capabilities, electrical biosensors have exceeded conventional detection methods.

In electrochemical biosensors, the reaction happens at the surface of electrodes where both the analyte and bioreceptor bind with each other. Bioreceptor in combination with transducer are the most important parts of electrochemical sensor. Sensitivity, selectivity and response time depends on the characteristics of these two components. Type of the material which is used for transducer, size and shape of the material are some of the factors that can affect the limit of detection. Based on the transducer that is used, electrical and electrochemical biosensors can be classified in three categories: amperometric, potentiometric and impedance-based [27]. They are also classified into labeled and label-free types depending on whether the analyte is labeled or not. Enzymes, nanoparticles, and fluorescent probes are common labels for biosensors [27]. Recently, electrochemical biosensors use carbon nanotubes as sensing elements due to their unique physical and chemical properties [28]. Because of high aspect ratio, electrical and thermal properties,

carbon nanotubes (CNTs) is one of the best materials for using as transducers in biosensor technology.

Because of small diameter in size (less than 10 nm), CNTs can be used as one-dimensional transducers [29-31]. In this case, diffusion takes place on the surface of CNTs that lead to interaction between analyte and bioreceptor. Different techniques are used in order to deposit CNTs, as transducer for electrochemical biosensors. They can either be transferred to the surface of electrodes [32] or can be grown directly between the electrodes [33]. In certain types of electrochemical sensors such as chemiresistive sensors, CNTs bind via non-growth reactions. In this case a solution containing CNTs conjugate with bioreceptor and fabricate a label free biosensor.

Bioreceptor is another important component in biosensor, that conjugates with transducer as one of the steps in the formation of biosensor. In the case of electrochemical biosensor made of CNTs, certain amounts of receptor molecules bind to the surface of CNTs through either covalent or non-covalent binding [34].

After conjugating bioreceptors to the transducer, biosensor is ready to target analytes. Based on literature reviews for electrochemical biosensors, there are many different types of receptors that are used for binding to analyte. DNA, protein and enzymes are three main receptors used in biosensors. Single stranded DNA binds to its complimentary strand during nucleic acid synthesis. Also, for protein applications, antibody recognizes its specified antigen. In the case of bacteria detection, CNT based biosensor have high limit of detection level for variety of analytes. For example, SWCNT based electrochemical biosensor can

detect *E. coli* O157:H7 at a limit of detection of  $10^5$  colony forming unit per milliliter (cfu/ml) [35], a limit of  $10^2$  PFU/ml for MS2 bacteriophage [35], 100 fM limit of detection for nucleic acids [36] and fM limit of detection for H1N1 virus [37].

### 1.3 *Escherichia coli* Biosensors

*Escherichia coli*, known as *E. coli*, refers to a group of bacteria commonly found in the intestines of humans and animals due to contaminated food or water [38]. Although many strains of *E. coli* are harmless; however, certain serotypes such as *E. coli* O157:H7, have acquired toxic trace during their evolution. Shiga toxic-producing *E. coli* or (STEC) is a term for all *E. coli* strains with toxic traces. STEC contamination is not rare. For example, serious complications of *E. coli* O157:H7 infection can lead to kidney failure. Water, beef, dairy products and even vegetable are common source of contamination. Incubation time is among 1 to 10 days whereas symptoms of infections starts normally after 3 days of exposure [39]. Elderlies and young children are more likely in danger of these infections. Some common types of diseases which are derived from *E. coli* are strokes, kidney dialysis and blood transfusion. The infection can be identified by laboratory testing and takes hours to weeks depending on different parameters such as source availability. This detection time is very important for those affected by the bacteria in order to decrease the life time of pathogens inside the body.

In United States, it is reported that annually around 73,000 illnesses and 2,100 hospitalizations occur because of *E. coli* contamination. In Canada the number is 4000 hospitalizations and 105 deaths [39]. Public Health Agency in Canada has reported that 4 million foodborne and waterborne

illness occur each year, and due to lack of monitoring, they are often misdiagnosed. This leads to expensive and complicated diagnostic procedures, in addition to high cost and long-lasting treatment. In other parts of the world with less drinking water, every year almost 1 out of 10 people become ill because of diarrheal diseases, estimating that 550 million people are ill and 230,000 of those are prone to deaths [40].

Detection and monitoring of water and food borne pathogens are of most importance to public health and relevant industries. Agriculture and food industry require the use of fast response, portable and cheap devices to monitor their sample for detecting pathogens more than other industries. Being able to detect the number of pathogens in current water sources, helps individuals avoid ingesting diarrhea-causing by bacteria such as *E. coli*.

*E. coli* is a rod-shaped bacterium with approximately 0.5  $\mu\text{m}$  width and 2 $\mu\text{m}$  length. Because of its relatively large size and rod shape structure, lower concentrations of *E. coli* expected to be detected by chemiresistive biosensors.

Several detection methods are currently being used for bacteria sensing. The current detection method relies on lab based bacterial culture that takes several hours to few days to test the samples. In this case, biosensors detect bacterial components such as DNA, RNA and enzymes. As it was mentioned earlier, the need for culturing the bacteria using different materials and methods in the lab make this technique time consuming and costly. Therefore, there is significant demands for biosensors that can detect whole cell of bacteria with good limit of detection in a short period of time. This is especially useful because the infectious dose of bacteria for many human pathogens is very low. In the case of *E. coli* O157:H7 it has been reported to be as low as only 10 cells per gram of food or environmental sample [41].

Significant researches have been done for detection of whole bacteria using impedimetric and optical methods. In this work a new technique has been developed for detecting *E. coli* K12 bacteria using chemiresistive biosensor made of multiwalled carbon nanotubes (MWCNTs). MWCNTs functionalized with magnetic nanoparticles, act as the transduction element and magnetically assisted printing is used to obtain a thin conducting strip. The sensing strip is functionalized with specific antibodies for target bacteria. Specific binding between antibody and bacteria is investigated by measuring the change in the resistance of the strip. A response time of ~ 2 minutes can be attributed to the sensor which makes our system a fast response sensor. The detection limit with whole cell is in the range of  $10^5$  cells/ml, whereas with the cell lysates, the limit of detection improves to  $10^3$  cells/ml.

## 2. Carbon nanotubes: properties and use in biosensors

### 2.1 Introduction

In this chapter, a brief background on carbon nanotubes and the process of magnetizing them to develop magnetic carbon nanotubes (mCNTs) is being explained. The functionalization of CNTs with carboxylic groups as well as synthesis of magnetic nanoparticles on the surface is demonstrated. The purpose of this work is to make a uniform strip printed of the mCNTs on the substrate by applying a magnetic field and also provide sites containing carboxylic groups on the surface of CNTs for binding Abs. Due to electrical properties of mCNTs they are capable of responding to external changes on their surface. This characteristic is a great advantage for biosensors in development of bacteria sensing that leads to enhance real time, on-site and portable CNT based biosensor.

Fabrication and surface modification process of mCNTs available in the literature will be provided, along with a summary of the principles and characterization techniques typically used for mCNTs biosensors.

### 2.2 Carbon Nanomaterials for Biosensing

Carbon based nanomaterials are one of the best known materials used in biosensor applications due to their novel properties [42-46]. Based on different hybridization states of carbon, it can bond to other atoms through different binding techniques. As shown in figure 2.1 graphite and diamond are two examples, formed due to different hybridization



state of carbon. Diamond which is well known for its mechanical properties and thermal conductivity, is formed when a carbon atom in its  $sp^3$  hybridized state shares four valence electrons with four neighboring carbon atoms [47,48]. On the other hand, graphite forms by sharing only three of the four electrons covalently with neighboring atoms, and the fourth is delocalized amongst all atoms. In this case, the carbon atom is at  $sp^2$  hybridized state [47].

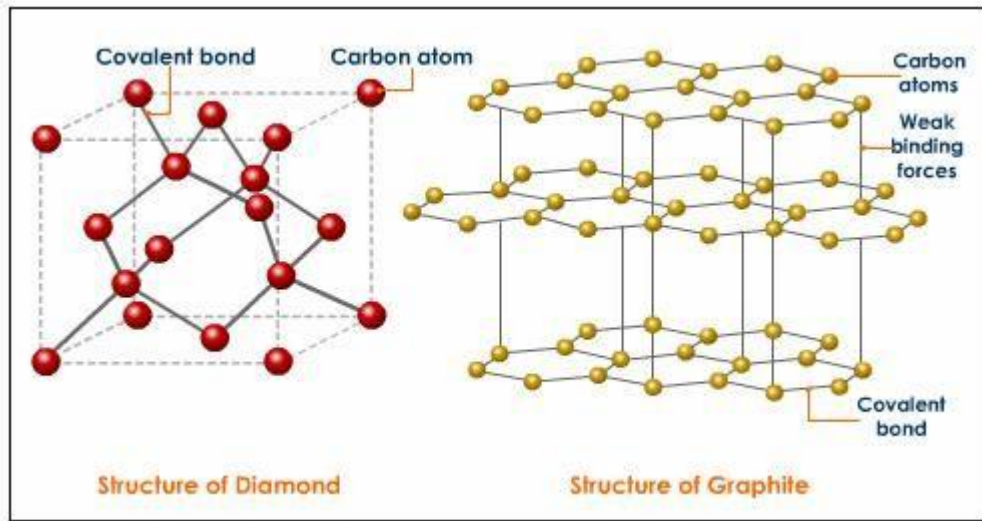


Figure 2.1: Carbon structure exhibiting different hybridization states:  $sp^3$  hybridized diamond (left) and  $sp^2$  hybridized graphite (right). Adopted from ref. 47

Graphite is a set of two-dimensional layers and is the most thermodynamically stable form of carbon at room temperature. Each layer consists of a hexagonal honeycomb structure of  $sp^2$  hybridized carbon atoms with a C-C bond length of  $1.42 \text{ \AA}$  [49]. Single layer of graphite known as graphene, bond via noncovalent van der Waals forces. These weak interactions between layers of graphite make the single graphene layers being chemically or

mechanically exfoliated. A graphene sheet can be rolled or distorted into other  $sp^2$  hybridized carbon nanostructures such as SWCNTs and fullerenes [50].

Because of this property that carbon atoms can find in different allotropes and exists as fullerenes, carbon nanotubes, and graphene which are 0-dimension, 1-dimension and 2-dimensions respectively, carbon nanomaterials have found their way in the field of biosensor as transducing element. In this scale, the properties of carbon nanomaterials are not only dependent on their atomic structures, but also on the interactions with other materials. Among different structures of carbon, CNTs have attracted significant attention due to their electrical and thermal properties, high mechanical strength, and enhanced optical and chemical assets.

### *2.2.1 Structures and types of CNTs*

Investigations done by Iijima in 1991 using high resolution transmission electron microscopy (HRTEM) for carbon nano-filaments led to the discovery of multiwalled carbon nanotubes (MWCNTs) [50]. Single walled carbon nanotubes (SWCNTs) have also been reported by Iijima in 1993 [50] and Bethune [51]. SWCNTs is a one-dimensional graphene sheet layer rolled into a cylindrical shape with a diameter of about 1-2 nm [50]. Double wall carbon nanotubes (DWCNTs) are similar to SWCNTs in terms of morphology but are significantly different to chemical resistance [52]. MWCNTs are made of multiple wrapped graphene sheets into concentric cylinders with a  $\approx 3.3$  Å interlayer distance and 10-80 nm in diameter [53]. In carbon nanotubes, each carbon atom forms three strong  $sp^2$  hybridized covalent bonds ( $\sigma$ -bonds) with three neighbouring atoms that have intersection angles of  $120^\circ$ .  $Sp^2$  hybridization combines a 2s orbital with two 2p orbitals in the carbon

atom. However, the third 2p orbital forms a relatively weak  $\pi$ -bond, which is commonly used for covalent functionalization of MWCNTs with external molecules. The three strong  $\sigma$ -bonds are mainly responsible for the unique properties of SWCNTs and MWCNTs [51].

Based on direction that the graphene sheet is rolled, different structures as well as different properties can be obtained for CNTs. To explain the geometry of CNTs, two unit vectors  $a_1$  and  $a_2$  and indices  $n$ ,  $m$  are defined as shown in figure 2.2. The lattice or chiral vector can be defined as:  $C_h = n_{a_1} + m_{a_2} = (n,m)$  where  $0 \leq |m| \leq n$ . The length of the chiral vector,  $C_h$ , is directly related to the diameter of nanotube. The chiral angle ( $\theta$ ) between  $C_h$  and  $a_1$  vector ( $0-30^\circ$ ) determines the structure of CNTs. The electronic properties of CNTs changes significantly with chiral angle from conducting to semiconducting [55]. If  $n=m$  ( $\theta=30^\circ$ ) CNT have armchair configuration. CNTs with  $m=0$  ( $\theta=0$ ) have zigzag confirmation. And finally, if  $n \neq m$  ( $0 < \theta < 30^\circ$ ) CNTs are called chiral [54].

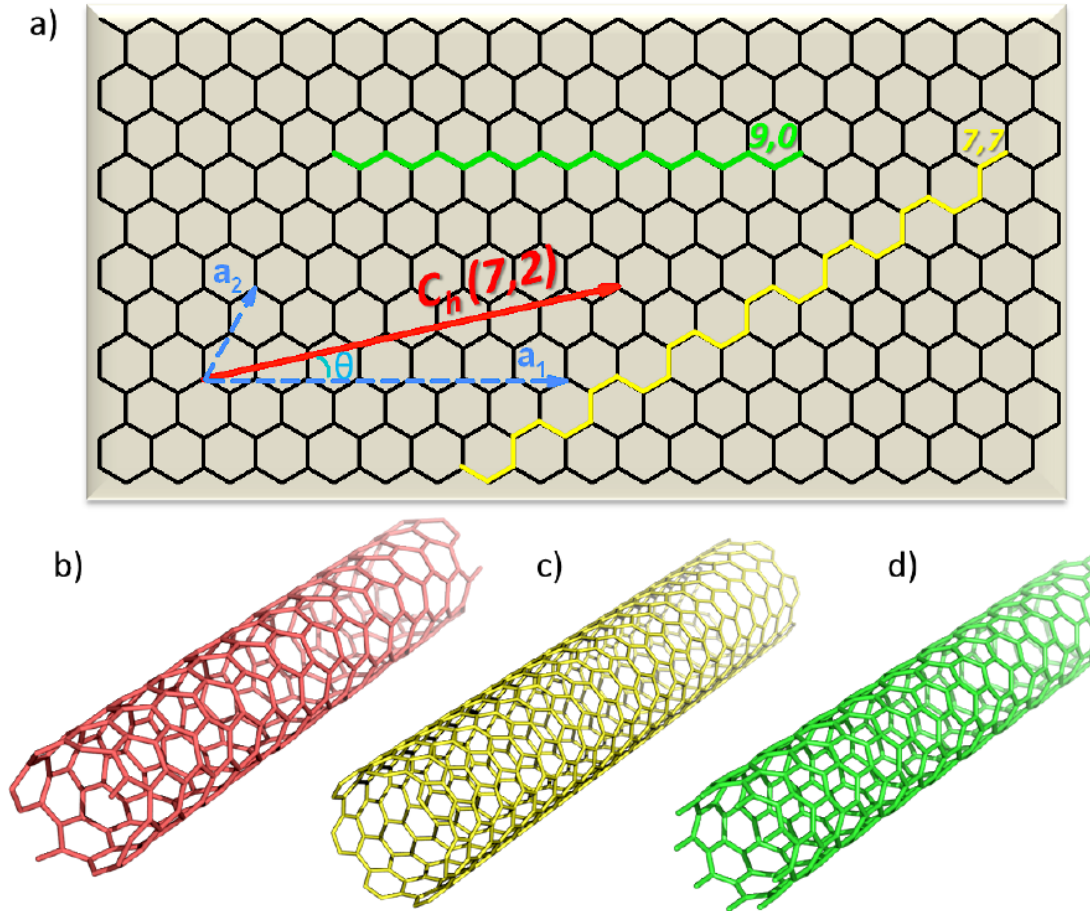


Figure 2.2: Physical structure of CNTs a) yellow and green lines represent armchair and zigzag configuration respectively.  $C_h$  is the chiral vector defined by unit vectors  $a_1$  and  $a_2$  and angle  $\theta$  b) chiral SWCNT- (7,2), c) armchair SWCNT- (7,7) and d) zigzag SWCNT (9,0). Adopted from ref. 47.

### 2.2.2 Properties of CNTs

High aspect ratio, high mechanical properties such as young's modules of 2 TPa [56], high surface area, and excellent electrical, thermal and chemical strength are the main properties of CNTs [57]. However, because they are forming out of graphite, CNTs are not very

reactive. Another factor that prevent CNTs, from reacting with other molecules is oxidation. CNTs are oxidized at temperature above 750 °C to the gas phase.

### *2.2.3 Application of CNTs*

CNTs can either be metallic, or semiconducting with small and large band gap [52]. MWCNTs are metal-like with a measured electrical resistivity of  $10^{-4}$  to  $10^{-3}$   $\Omega$  cm [58]. Some other significant characteristics of CNTs are high thermal conductivity, high thermal stability, high surface area, low density and superior mechanical properties [53,58,59]. Due to these properties, CNTs are used in many applications such as sensors [60,61], nanoelectronics [62,63], biomedicine [64-67], fuel storage [68,69], high-strength materials, conductive suspensions [70] and scanning microscopy tips [58].

CNTs as mentioned before, have become one of the best known materials for biosensing since their discovery. Physical and chemical properties of CNTs make them well suited for sensing applications. Because of their high sensitivity to surrounding environment, they are a good choice of transducer for electrochemical biosensors [71]. The reason for this sensitivity is carbon atoms within the nanotube that are located on the surface, which interacts with all atom on the surface area. CNTs can be either metallic or semiconducting, based on chirality. For example, semiconducting SWCNTs are being used in field effect transistors (FETs), whereas MWCNTs are potentially useful as transparent conductors [72,73]. SWCNTs maintain a high conductivity along their length, makes them ideal electrode nanomaterials and nanoscale FETs [74-76].

CNTs have highly sensitive optical properties such as characteristic Raman signal [77] and can be used as a nanoscale biosensor inside cells or dispersed through a system in order to capture the small amount of analyte present in the system [78]. In addition, CNTs act as a support to carry a biomolecule such as antibodies [79] or be used as functional element for label free electrical detectors [80]. In electrochemical enzyme biosensors CNTs are directly plugged in to individual redox enzymes as a transducer [81]. Decrease in current due to electrochemical reactions are transferred through the nanotubes to the metal surface and, can be detected using voltammetry or amperometry techniques [82]. FET sensor used SWCNTs for the first time for detection of gases [83] followed by detection of chemical species in liquids. Finally sensing of biological molecules such as metabolites, proteins and nucleic acids happened by using catalytic and affinity based CNT-FETs [84-86]. In the case of molecular detection, FET biosensors based on SWCNTs use a single nanotube or a combination of several nanotubes for detection of single molecule [87]. In the case of having single nanotube, better sensitivity can be obtained in comparison with having a combination of several nanotubes. On the other hand, FETs with several nanotubes provide better reproducibility. Although these sensors show good sensitivity however because of expensive and complicated instrument, it is difficult to use them for mass production.

#### *2.2.4 Synthesis method*

CNTs were initially synthesized by arc discharge method [88]. Nowadays chemical vapor deposition (CVD) is the most relevant technique for synthesizing CNTs. Lower cost, high purity, large growth area, and ability for large scale production are the advantages of this technique. During this process, hydrocarbon gases such as ethylene decompose on a hot

metallic substrate ( $\sim 1000^{\circ}\text{C}$ ) with catalytic properties at atmospheric pressures to sustain CNT growth on the metallic catalyst. The catalyst could be deposited on a substrate as solid or be injected as a gas [89-91]. Recently, plasma enhanced CVD (PECVD) has replaced thermal-based CVD, since it reduces the decomposition temperature of the hydrocarbon gas ( $\sim 550^{\circ}\text{C}$ ) [90-92].

As mentioned earlier, CNTs are being produced using different methods such as CVD, laser ablation and arc discharge which are called growth method. The final product contains a mixture of CNTs, catalysts particles and amorphous carbon. Additionally, the nanotubes in the mixture are not identical and represent different length and chirality therefore have different properties. Based on the CNTs hexagonal structure and their quantized wave vector values, metallic and semiconducting CNTs are synthesized mainly at a 1:2 ratio [93]. Because of these limitations, modifying synthesis process of CNTs for using as transducer plays an important role in developing a sensor with good reproducibility and device performance.

#### *2.2.5 Challenges in handling CNTs*

CNT has a one-dimensional anisotropic structure. Van der Waals attractions between the surface of CNTs and/or Brownian motion in the dispersing medium make CNTs entangled and randomly orientated. This randomness reduces their application efficiency [94-95]. It is the reason why there is a reproducibility issue with CNTs based devices. CNTs are hydrophobic materials due to their non-polar honeycomb structure. Therefore, when it comes to solution based technique for fabrication of CNTs based device, this hydrophobicity reduces the compatibility of CNTs with many dispersing mediums,

including polar solvents and polymers [96]. To avoid this, CNTs are coated with surfactants and subsequently sonicated for dispersion which generally affect the electrical properties of the CNTs because of mechanical cleavage under sonication [97]. Also, coating SWCNTs with other materials decreases the sensitivity of the transducer, as they are no longer directly exposed to the analytes. CNTs are diamagnetic materials, like graphite, with a diamagnetic susceptibility ( $\chi$ ) of  $-5.9 \times 10^{-6}$  emu g<sup>-1</sup> [98,99]. Finally, CNTs are commercially produced in the powder form. This is a challenge for manipulation and control process of CNTs that limits their applications. Thus, the main problems for CNTs based biosensors are the inability to control properties of as grown CNTs as well as possible damaging occurs during solution based fabrication.

### 2.3 Functionalization of CNTs Biosensors

Functionalization is introducing external molecular groups on the surface of CNT in order to improve its physical and chemical properties [100]. Functionalization is required for certain applications of CNTs such as biosensing to modify sensitivity, specificity, reproducibility and biocompatibility depending on analyte, receptor and transducer. mCNTs become selective to a specific molecule by attaching the corresponding receptor to its surface. The bonding between CNTs and bioreceptors happens thorough covalent and non-covalent method. In non-covalent binding a weak bond like Van der Waals force take place between CNTs and molecules. The advantage of this method is that the surface of CNT is not significantly affected by the reaction. In covalent bonding, defect sites are presented on the surface of CNTs due to the stable hybridized C-C ( $\sigma$ ) bonds. These defect sites make the CNTs susceptible to attack by reactive molecular group [100]. For example,



oxidizing CNTs with  $\text{HNO}_3$  [101-107], and ( $\text{HNO}_3$  or  $\text{H}_2\text{SO}_4 / \text{H}_2\text{O}_2$ ) [104,106] forms  $\text{COOH}$ ,  $\text{C=O}$ , and  $\text{C-OH}$  groups which are covalently bonded to the surface of CNTs. Attaching nanoparticles (NPs) to functional groups takes place using a further step in which covalent bond form directly by changing the carbon atom hybridization from  $sp^2$  to  $sp^3$  or indirectly by chemical transformations of previously generated functional groups [103,108].

The degree of functionalization for different locations of CNTs is different due to presence of active sites. Also, by decreasing the diameter of CNTs their curvature increases which leads to more chemically reactive sites [109].

## 2.4 Magnetized CNTs-based sensors

CNTs can be functionalized with magnetic nanoparticles by using physical entanglement, covalent and non-covalent binding. This helps manipulating CNTs inside different dispersing medium by using external magnetic field.

### 2.4.1 Classification of Magnetic Materials

Based on magnetic properties and response to magnetic field, materials are classified into five different groups which are: (1) diamagnetic, (2) paramagnetic, (3) ferrimagnetic, (4) ferromagnetic, and (5) antiferromagnetic as shown in figure 2.3. Carbon and noble gases are an example of diamagnetic materials that have a negative susceptibility ( $\chi_M$ ) in the order of  $10^{-5}$  and very weak relative permeability. Electrons are coupled in diamagnetic materials and their net momentum is zero. The reason for having negative susceptibility is that in the presence of magnetic field, changes in the magnetic moment is based on Lenz

theory. Based on this theory, an induced electric current, flows in a direction such that the current opposes the change that induced it. Therefore, by increase or decreasing the intensity of induced field, velocity of electrons is in a way that reduce the effect of external field [110]. Paramagnetic materials such as oxygen have a low and positive relative permeability. In this type of materials, magnetic momentum of particles is not zero but they are arranged in such a way that the net magnetic momentum is zero. By applying magnetic field only few of the magnetic moments will be in the same direction with magnetic field. Ferromagnetic materials tend to align the magnetic momentum of nearest atoms even in the absent of magnetic field. In this type of materials, particles have a non-zero value of magnetic momentum and by applying magnetic field, will be aligned in the direction of applied field. Ferromagnetic materials have high positive susceptibility and relative permeability ( $10^2$ - $10^5$  emu  $g^{-1}$ ) so that all magnetic moments are equal and parallel. Iron, nickel and copper are three elements that have ferromagnetic properties [110]. Anti-ferromagnetism exists only in chromium, where magnetic moments have net positive value but are antiparallel in a way that neutral the total magnetization. In Neel temperature, anti-ferromagnetics behave like paramagnetic materials. Below this temperature their magnetic property increases [110].

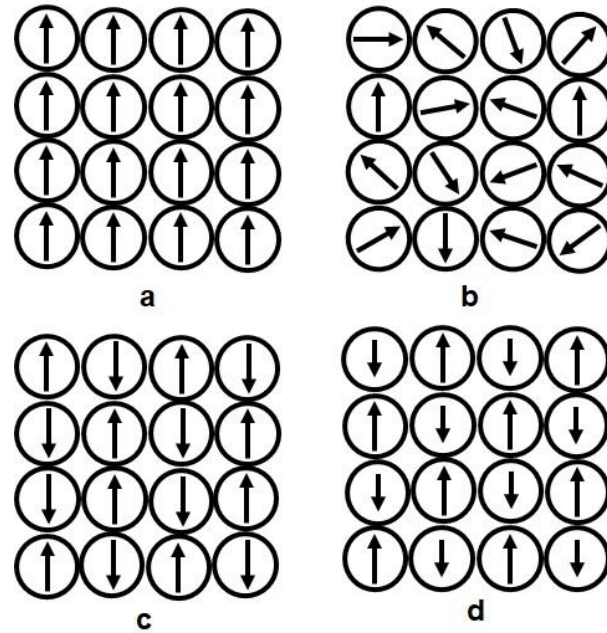


Figure 2.3: Different types of magnetism: (a) Ferromagnetism, (b) Paramagnetism. (c) Anti-ferromagnetism, and (d) Ferrimagnetism.

In Ferrimagnetic materials, although magnetic moments are divided to two or several antiparallel sections, however total magnetic moment has a large value same as ferromagnetic materials. The temperature which instantaneous magnetization disappear in ferrimagnetic materials is called Neel ferrimagnetic temperature [110].

#### 2.4.2 Magnetic domains

Magnetic moment is a part of magnetic material where all the magnetic domain in this part are parallel. Magnetic vector in each domain is different from its neighboring domain. The arrangement is in such a way to decrease the magnetic energy to its minimum level. Magnetic domains are formed due to decrease in magnetic energy. In each magnetic domain, momentums of each magnetic atom due to of interactive interaction are in the same orientation.

In ferromagnetic materials, momentum in each domain are in the same direction. However, in ferrimagnetic materials, magnetic moments of each domain are anti-parallel.

#### 2.4.3 Magnetism in small dimensions

By reducing the particle size, number of magnetic domains decreases until reaching to a point that in each domain we have one magnetic domain. For ferromagnetic and ferrimagnetic materials, reducing particles sizes below a critical dimension ( $D_c$ , 15-150 nm) changes the material containing multi-magnetic domains into a single domain (figure 2.4) [110]. For particles below critical domain, coercive force is zero. Due to thermal fluctuation, super-paramagnetic phenomena occur. Super-paramagnetism is a special case of such a material when the particle size is lower than the superparamagnetic diameter ( $D_s$ , few nm). In this case, the particle consists of a small single domain that can be conceived as a single massive paramagnetic atom. Here, the coercivity is zero and upon removal of the applied field there is no residual magnetization inside the material [110].

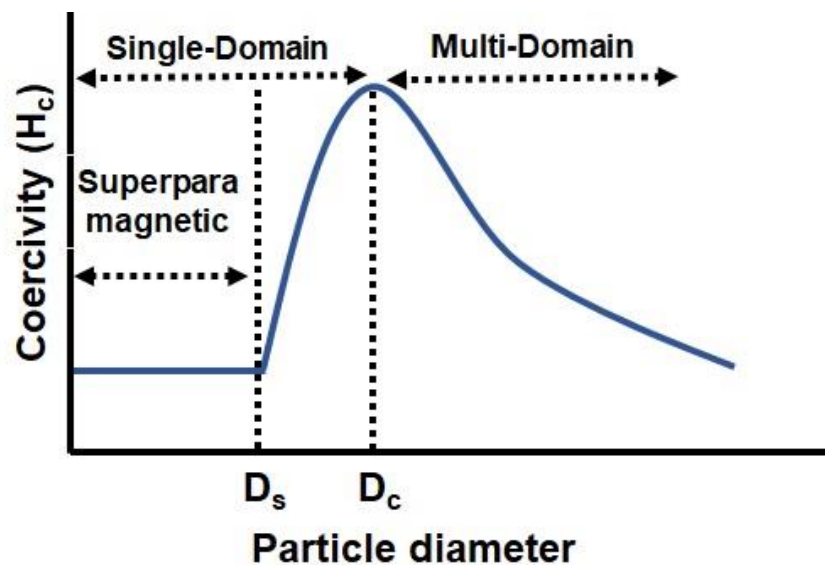


Figure 2.4: The relation between the coercivity and the particle size.

#### 2.4.2 *Magnetic Nanomaterials*

Any reducing the size of magnetic materials and reach to less than 100 nm, the magnetic material changes to a magnetic nanomaterial. One major characteristics of magnetic nanomaterials is higher surface-to-volume ratio and they can synthesized through several physical and chemical methods [110]. Because of their small sizes (few nm), magnetic nanoparticles (MNPs) are expected to be individually superparamagnetic [111].

#### 2.5 Magnetization of Carbon Nanotubes

Providing magnetic nanoparticles (MNPs) on the surface of CNTs via either covalent or non-covalent functionalization is called magnetization of CNTs. Introduction of MNPs with a high relative permeability to a diamagnetic material that has almost zero permeability leads to a hybrid material with intermediate magnetic properties. Magnetization is a suitable way to align and manipulate CNTs under an applied magnetic field e.g., by immersing them in a liquid prepolymer containing dispersed magnetized CNTs (mCNTs) as it experiences an applied magnetic field [112-113]. The magnetic nanoparticles that attach to a CNT surface provide new surfaces that are more compatible with dispersing mediums. They can be used to overcome the high contact electric resistance that arises due to the anisotropic behaviour of CNTs, and enhance their mechanical properties by assisting with mechanical load transfer [114].

In bulk materials, the superior properties of CNTs can be leveraged by dispersing them in a continuous matrix to form a nanocomposite [115]. Since CNTs are a quasi-one dimensional, their properties are best exploited by aligning them along their longitudinal

axes [116-118]. mCNTs are utilized in many applications including wastewater treatment [119,120], phase separation [121], biomedical applications [122], drug carriers [123], and microwave absorbers [124].

In order to commercialize the mCNTs based biosensors for bacteria detection from proof of concept, more research progress needs to be done regarding study the mechanism of electrical sensing as well as characterizing the interactions between different components of biosensors. One way to have reproducible sensor is measuring pH of mCNTs in controlled environments and compare with each other, then use for detecting bacteria. This helps to understand sensing mechanism and reliable quantification.

## 2.6 mCNTs Biosensor: Background

From the first CNTs based biosensor experiment reported in 1998 [125,126], there has been significant progress made towards characterizing CNTs as well as implying them into working devices. Many researches have used SWCNTs transistor type device in order to sense a variety of chemical and biological species. Although there have been valuable results obtained from most of these studies in this area, however the overall mechanism is still missing and needs to be investigated. For example, the mechanisms which create electrostatic interactions between transducer, biological species and device electrodes have not been completely understood. The lack of these information is one of the reasons for bringing different hypothesis between research groups till this date [127,128]. Different industries and organization such as agriculture and pharmaceutical industries rely a lot on techniques based pathogens detection [27]. Hence, to commercialize CNTs based biosensor

in clinical application, such as the bacteria detection, process in which bioreceptor binds with transducer and the interactions that happens has to be more studied.

Rather than electrostatic interaction, different hypothesis proposes higher sensitivity in small dimensional sensors [36] According to literature, theoretically there is a 5-10 times increase in sensor sensitivity because of electrostatic properties of transducer in small dimension. To explain the reason for higher sensitivity in small dimensional sensors, kinetics of diffusion should be taken into consideration [36]. However, this theory still requires more study in order to define the kinetics behaviour of nanomaterial based biosensors.

#### *2.6.1 Sensing mechanism of CNTs-based biosensor*

As mentioned earlier, one of the applications of CNTs based biosensors is detection of biomolecules in solution using electrochemical technique. However, the mechanism is still under question for scientists, which is a major drawback of using these sensors. Until now, there are five hypotheses for sensing mechanisms. They can be classified to electrochemical doping reaction, coupling mechanism, changes in the charged species, electro gating mechanism and Schottky diode (SB) mechanism [129]. These four techniques are based on binding between bioreceptor and target molecules, results in a change in the properties of CNTs. Some characteristics such as resistance, voltage and current of the transducer in a CNT-based biosensor is being affected. To figure out the mechanism beyond this process, there should be more studies on the different techniques and their effect on the reaction.

There are differences in the way each sensing mechanism work when a change occurs on the surface, consequently affecting CNTs electrical characteristics. The mechanisms investigate the effect of binding between analyte and bioreceptor on current by analyzing response in a current-voltage curve in a fixed potential. Band gap energy of CNTs also measured to study the effects on surface potentials. In this section, several hypothesis are provided to distinguish various kinds of techniques for analysing them and figure out where to apply them as well. Here, electrochemical doping reaction and electro-gating mechanism are being discussed.

#### *2.6.1.1 Electro-gating mechanism*

Based on this theory, there is a net charge exists in the nature of every molecule and is due to of chemical properties of molecule and chemical parameters in the suspension such as kind of ion and amount of pH. [129]. By adding analyte to the sensor, the interaction between biomolecules which contain a negative charge and CNTs, results in a change in potential on the surface of transducer. In this case, the biomolecule, modify the surface potential of transducer which is called electro gating mechanism. The process is based on binding molecules on the surface of CNTs and change in the outer layer electron gap energy [15]. In this mechanism the current is fixed and the potential of the transducer is the only value which is changed.

Molecular weight of reagents exist in the analyte is one of the main parameters determine the mechanism. The analyte which is in contact with CNTs, affects the certain amount of the CNTs. The length of the biorecognition system in contact with the analyte and is experiencing the electro gating mechanism is called Debye length [15]. In this case, the



electrostatic mechanism affecting on the other parts of CNTs which is not in contact with the analyte does not have any effect on the response of the biosensor. Debye length can be calculated from the equation which is mentioned below.

$$\delta = \sqrt{\frac{\epsilon_0 \epsilon_r \chi_B T}{2 N_A e^2 I}}$$

Here,  $\epsilon_0$  and  $\epsilon_r$  are permittivity in vacuum and relative permittivity of the analyte respectively,  $\chi_B$  is referred to Boltzmann's constant, T is the temperature in Kelvin,  $N_A$  is Avogadro's Number, e is the electron charge and I is the molecular weight of the ions in the analyte. The formula for the Debye length clearly states that increasing molecular weights of ions in the analyte reduces the Debye length and therefore the effect of electro gating mechanism. Thus, in order to obtain a good response out of the sample using this mechanism the weights of the ions in the solution is preferred to be low [15]. By tuning the value of Debye length, which means adjusting it to the length of antibodies functionalized on the surface of CNTs, binding between antigen and antibody can be detected using electro gating mechanism [131].

#### *2.6.1.2 Electrochemical doping*

Carbon nanotubes have the ability to accommodate electrons from different atoms in their structure. There will be unique features with the new structure which is developed such as high conductivity and super paramagnetism property [132]. Based on this mechanism, by doping the electrons from other materials in the form of gas and liquid, electrical properties of CNT changes which lead to generate a response from the sensor. This mechanism

involves binding between CNTs and other reagents in the analyte [133]. Reduction and oxidation of material is in combination with the chemical doping [134].

Investigation done on the two mechanism that was discussed mostly comprised of applying small samples as the target material like protein. In the case of big molecules like *E. coli*, the principle is not the same. Like the electro gating mechanism sensing, one of the major changes in the case of detecting big particle is the molecular weight of the analyte. Here, diffusion coefficient for large molecules is smaller in comparison to smaller particles [135]. This small diffusion for larger particles results in having higher signal. Therefore, the expected outcome for bacteria detection using CNT-based sensor is that higher limit of detection can be obtained.

## 3. Developing a biosensor printed strip out of MWCNTs

### 3.1 Introduction

In this chapter, functionalization of MWCNTs via covalent binding is being explained. Attaching magnetic nanoparticles (MNPs) to the surface of CNTs, help to provide a uniform printed strip in the presence of a magnetic field. Fabrication of the biosensor consist of 5 different steps such as: (1) magnetizing the MWCNTs, (2) preparation of bio-ink with mCNTs, (3) printing the bio-ink on the substrate, (4) design and attaching flow cells on the dried sensing strips and (5) functionalizing sensing strips with antibodies. Magnetizing the MWCNTs is performed as per prior reported work [134,135]. In this work, in order to make the biosensor out of bio-ink, strips are formed by printing the ink first and functionalizing after being dried in ambient temperature. The probability of Abs being present on the surface of the sensing strips in this procedure is higher in compare to functionalizing the mCNTs with Abs during the ink preparation stage. This helps in producing a more sensitive sensor with a better limit of detection.

### 3.2 Methodology

#### 3.2.1 *Materials and Reagents*

Multiwalled carbon nanotubes (MWCNTs) produced by chemical vapor deposition technique with purity > 95%, outside diameter of 20-30 nm, inside diameter of 5-10 nm and lengths between 0.5-2  $\mu\text{m}$  were purchased from US Research Nanomaterials, Inc. Ferric chloride hexahydrate ( $\text{FeCl}_3 \cdot 6\text{H}_2\text{O}$ , 97–102%) and ferrous chloride tetrahydrate ( $\text{FeCl}_2 \cdot 4\text{H}_2\text{O}$ , 98%) was procured from Alfa Caesar. Nitric acid ( $\text{HNO}_3$ , 68-70%) and

ammonium hydroxide (NH<sub>4</sub>OH, 28-30%) was purchased from CALEDON Laboratory Chemicals. Anti-*E. coli* rabbit polyclonal antibodies (Abs) and Secondary Ab, a fluorescein isothiocyanate (FITC)-conjugated goat antirabbit IgG H&L, used as a fluorescent marker were purchased from Abcam. *E. coli* K12 and *Bacillus Subtilis* were donated from New England Biolabs. Tween20, 1-ethyl-3-(3-dimethylaminopropyl) (EDC), Luria Bertani (LB) microbial growth media powder and Phosphate buffered saline (PBS) solution purchased from Sigma-Aldrich. N-Hydroxysuccinimide (NHS) was purchased from ThermoFisher Scientific. 3M 9472LE double sided adhesive tape was obtained from Muir tapes & adhesives. LB broth was prepared by diluting 10 g of the powder in 500 ml of distilled water and autoclaved for use as the media. 1x PBS used in washing and suspending bacteria was sterilized in an autoclave.

### 3.2.2 *Synthesis of magnetized carbon nanotubes (mCNTs)*

Magnetic nanoparticles were attached to the surface of MWCNTs using coprecipitation method as mentioned in our previous work [136,137]. Briefly, MWCNTs are activated by dispersing in nitric acid and sonicated for 4 hours to create sites containing carboxylic groups. The activated MWCNTs are then dispersed in the solution containing iron salts. With the addition of ammonium hydroxide that acts as a precipitant, magnetite (Fe<sub>3</sub>O<sub>4</sub>) nanoparticles nucleate at the active sites of MWCNTs tethered to the carboxylic groups to produce the mCNTs.

### 3.2.3 *Bio-ink fabrication*

mCNT ink preparation is the first step in fabricating the biosensor out of mCNTs. 7 mg of mCNTs is dispersed in 10 mL of distilled water (DW). The solution then ultrasonicated two times for overall 10 minutes with a duty cycle of 10 seconds and 30% amplitude. This will help mCNTs to uniformly disperse inside the solution and form a suspension. Tween20, a non-ionic surfactant is added to the suspension at 0.1% v/v and rotated on a roller for 30 minutes at 25 rpm to coat all the surfaces of mCNTs (Figure 3.1b). Adding Tween20 in addition to make the prints out of mCNT suspension more uniform, help blocking the surface and avoid any non-specific bindings happen between antibodies which will be coated on the surface with bio-analytes. The suspension is then centrifuged at 3600 rpm for 5 minutes to harvest the mCNTs. After pelletizing the mCNTs at the bottom of the tube, supernatant is removed and 10 mL of DW added to disperse the mCNTs. We call this step washing and repeats for three consecutive times, using same parameters for centrifuge. Finally, by resuspending in 500  $\mu$ L of DW, mCNTs bio-ink is made. In this work, the bio-ink keeps in the 4°C fridge for overnight before printing. Figure 3.1 shows bio-ink preparation and printing of the ink on a glass slide.

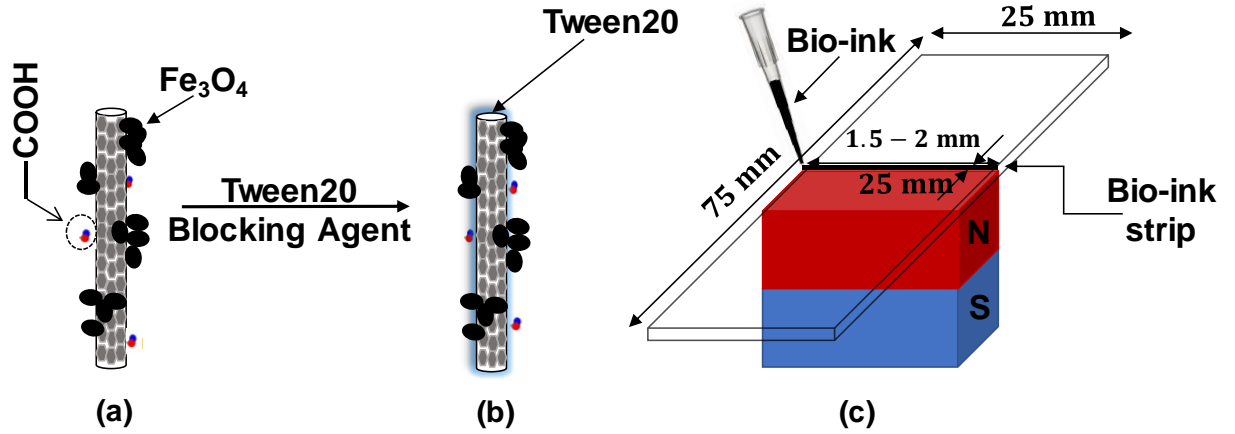


Figure 3.1: Schematic of the steps involved in ink preparation and printing: a) magnetized carbon nanotubes with available carboxylic groups on the surface, b) addition of Tween20 to avoid agglomeration and c) magnetically assisted printing of the ink on a glass slide to form a thin conducting strip.

### 3.2.4 Printing the bio-ink on the substrate

In order to make a bio-strip out of bio-ink, a glass microscope slide with 75mm length and 25 mm width chose as substrate and is placed on a magnet with the magnetization direction being through the thickness of the glass slide. For each printed strip, 10  $\mu\text{L}$  of the prepared bio-ink is deposited with pipet along the edge of the magnet. The highest magnetic field gradient at the edge of the magnet concentrates the mCNTs to a thin conducting strip of width 1.5 – 2 mm and 25 mm length as illustrated in Figure 3.1(c). Strips are then air dried over the magnet for approximately 15 minutes and mCNTs adhere to the glass substrate by electrostatic and van der Waals forces.

### 3.2.5 Flow cell design

In order to functionalize the bio-strips, a flow cell is designed and attached over the printed strip to have controlled flow of liquid. The flow cell preparation step is illustrated in Figure 3.2 (a-b). First, a 3M double sided adhesive tape is patterned and cut into 20 mm x 20 mm piece with a slit of 4 mm using Cricut cutter. This patterned tape is attached to a diced glass slide with the same dimensions which is then attached over the printed and dried strip. The slit in the tape makes the flow cell as shown in figure 3.2(a). The height of this flow cell is approximately 40  $\mu\text{m}$  which is the thickness of the adhesive tape. The calculated volume of flow cell is 3.2  $\mu\text{L}$ . Flow of liquid through the flow cell is primarily due to wetting and capillary forces. Flow cell enables washing, reduces evaporation, control exposure of strip to different solution and provide a reproducible wetting area of the strips.

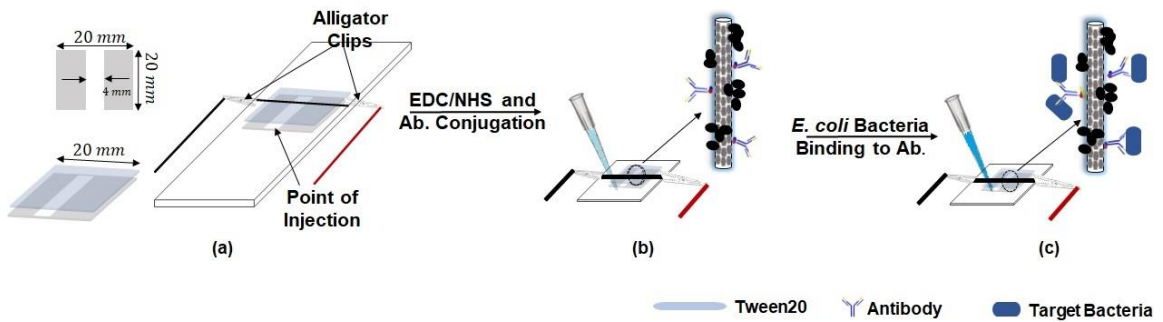


Figure 3.2: Functionalization of the bio-strip: (a) fabrication of flow cell over the sensing strip, (b) antibody immobilization and (c) specific binding of bacterial cells with the specific antibodies on mCNTs.

### 3.2.6 *Functionalizing the strips with Abs*

Antibodies conjugate with mCNTs through COOH groups present on the surface. One way to increase the chance of binding between antibodies and mCNTs is using crosslinkers. In this work, EDC/NHS chemistry have been utilized for binding Abs to the available carboxylic group sites on the surface of the mCNTs. After attaching flow cells to the bio-strips, a solution containing a mixture of 0.1 M NHS and 0.4 M EDC is prepared in DW and 10  $\mu$ L of the solution is injected on to the dry strip. The strip is then left to incubate for 15 minutes and subsequently washed twice with 15  $\mu$ L of DW. The antibody solution is then immediately added to the strip. The higher amount of Ab is supposed to provide a sensor with more sensitivity with lower limit of detection. In this work 0.1 mg/ml of *E. coli* K12 Ab was used for each strip (Figure 3.2 b). The whole process should not take more than 30 minutes because, EDC/NHS loses its linking properties in a short period of time. and incubated at 4°C overnight to obtain a functionalized sensing strip.

## 3.3 Results and Discussion

### 3.3.1 *Optical and Electrical characterization of printed sensing strip*

Optical and electrical characteristics of the sensing strips are evaluated to measure the variation in the printed strips. Variation in the width of printed strips is measured using a stereo zoom trinocular optical microscope (VWR). Dried and printed strips are imaged and the width at six different locations along the length of the strips are processed in ImageJ. Figure 3.3 (a) shows the average value of the width from six locations measured for 7 different sample of the sensing strips. The average width of the strips varies from 1,570-



1,880  $\mu\text{m}$  with the maximum standard deviation of 3.5%. This implies that using 10  $\mu\text{L}$  volume of bio-ink for each print provides a continuous and a fairly uniform width along the length of the strip.

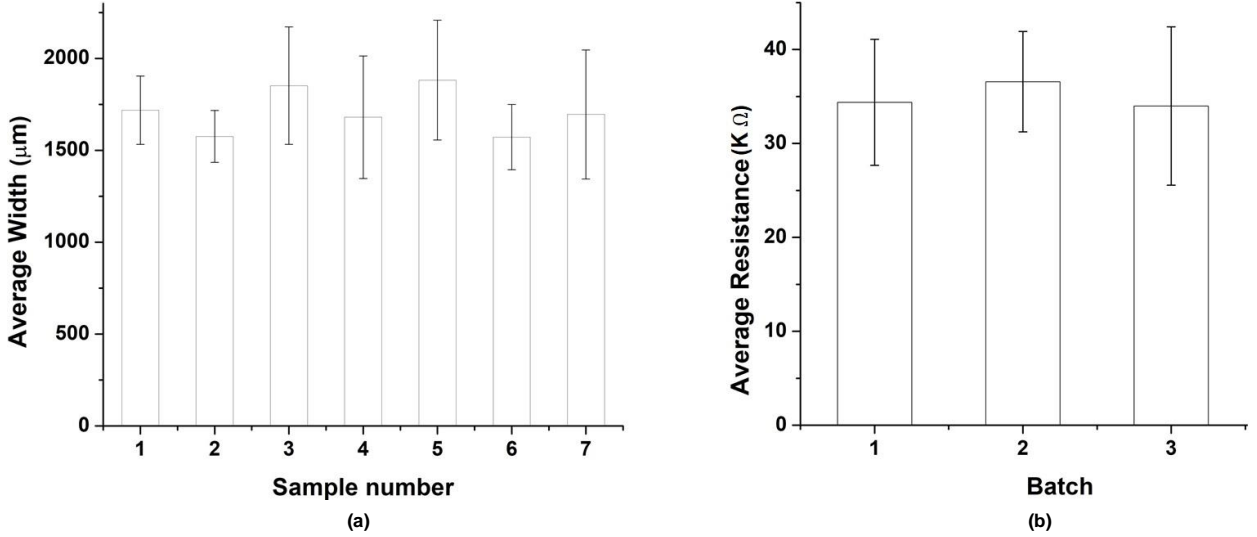


Figure 3.3: Characterization of the printed sensing strips: a) average width of printed strips measured with a microscope, b) average resistance of functionalized strips measured using multimeter.

Resistance of the functionalized sensing strips are measured using a digital multimeter. Three batches of strips prepared on different days are used for this experiment. For each batch, resistance of 7 strips are measured by connecting the multimeter probes to the either side of the printed strips. The sample and batch variation of the electrical resistance is shown in Figure 3.3 (b). The spread of the average resistance is between 23.4 to 48.24  $\text{k}\Omega$ . The maximum standard deviation among the batches is 8.4%. The variation in the electrical resistance could be attributed to factors such as (1) variation in the width and thickness of the sensing strip and (2) inhomogeneous distribution of mCNTs across the strip. One way

to improve the variation of the strip is to keep the mCNTs suspension overnight and print the next day. It has been proved that more uniform print can be obtained in this case. In order to avoid inhomogeneous distribution of mCNTs, increasing the sonication time can be a method to consider. Also, applying bath sonication before printing the strips is another technique which can be considered.

### 3.3.3 *Fluorescent microscopy imaging*

To confirm the binding of Abs onto the surface of mCNTs, a fluorescing secondary Ab with affinity to the primary Abs is used and bio-ink is imaged with a fluorescent microscope. 9 mL of bio-ink solution is prepared as described in section 3.2. After that, 1 mL of EDC/NHS solution containing 0.1 M NHS and 0.4 M EDC, is added to the bio-ink solution and left to rotate on a roller for 15 minutes at 25 rpm. The suspension is then washed with DW, applying the same process of washing in section 3.2. 1 mL of the solution is kept aside as the control and the antibody solution is immediately added to the rest of the solution and placed on the roller for 1 hour at 25 rpm to let the Abs conjugate with the surface of mCNTs. The conjugated suspension is then thoroughly washed using 1x PBS instead of DW. In the last step, 3 mL of the solution is pipetted in 3 separate tubes and different concentrations of secondary Ab is spiked to each tube. FITC-conjugated goat antirabbit IgG H&L, is used to label the antibody conjugated with mCNTs. Figure 3.4 shows the results of binding varying amounts of FITC labeled fluorescent Ab to the bio-ink. The left side of the image represents the bright field image and the right side is the fluorescent microscopy image. Each of the black particle in the bright field images in figure

3.4, is an mCNT aggregate that constitutes the ink. The presence of fluorescence on the aggregate of the mCNTs indicate the successful conjugation of the primary Abs on the surface of mCNTs. Figure 3.4 (a-c) shows images for the Abs immobilized on mCNTs and conjugated with FITC labeled fluorescent Ab with concentrations of 50  $\mu\text{g/ml}$ , 10  $\mu\text{g/ml}$  and 1  $\mu\text{g/ml}$  respectively. Figure 3.4 (d) is the control without primary Abs on the mCNTs surface. The negative control sample in figure 3.4(c), does not show observable amount of fluorescence, indicating the low non-specific adsorption of the FITC secondary Ab. Within figure 3.4 (a-c), the intensity of fluorescence decreases in correlation with the decreasing amount of secondary antibody indicating the specificity of fluorescent secondary antibody and the presence of primary antibody on the mCNTs.

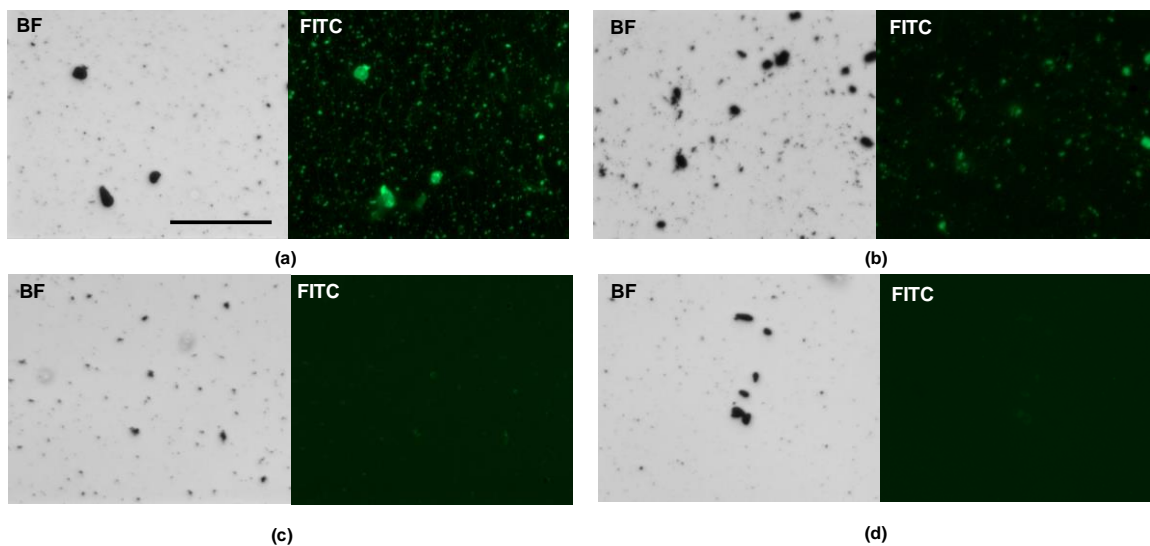


Figure 3.4: Visualization of *E. coli* Abs. immobilized on the surface of mCNTs. Brightfield and fluorescent microscopy images of FITC labelled secondary antibody for different concentrations of (a) 50 $\mu\text{g/ml}$ , (b) 10 $\mu\text{g/ml}$  and (c) 1 $\mu\text{g/ml}$ . The fluorescence indicates the successful conjugation of FITC labelled antibody with the primary *E. coli* Abs covalently

bonded to the surface of mCNTs. Panel (d) shows the effect of fluorescent Abs on the ink without any primary Ab.

### 3.4 Conclusion

A new method for developing chemiresistive biosensor has been produced. In this case, biosensor is made out of bio-ink which is printed on a glass substrate. Bio-ink suspension consists of CNTs which are decorated with magnetic nanoparticles in order to concentrate on the substrate when printed under the influence of magnetic field. To provide a uniform dispersion as well as printing uniform strips, Tween20 which is a surfactant also added to the suspension to cover all the surface of mCNTs. Optical results from printed strips proves that different strips have the width between 1.5-2 mm. Resistance of strips are almost in the same order. Conjugating Abs on the surface of mCNTs happen after an overnight incubation of strips inside the 4°C fridge. We call this method, post functionalizing. In this case results of fluorescent optical microscopy also shows that Abs bind to the surface of mCNTs. By providing more carboxylic groups on the surface of CNTs, concentration of Abs on the surface will be higher. In this case better sensitivity is expected by the sensor.

## 4. mCNT based chemiresistive sensor for bacteria detection

### 4.1 Introduction

In this chapter, experimental procedure is presented to discuss the sensor application of mCNTs synthesised via covalent functionalization. Multiwall carbon nanotubes decorated with magnetic nanoparticles (MNPs), dispersed in DW constitutes a biological ink which is both magnetoresponse and electrically conductive followed by conjugating with Abs. In this work the process of making a biosensor to detect different concentrations of bacteria in water samples is being discussed.

### 4.2 mCNTs based biosensor for detecting bacteria

Possible applications have arisen in recent years for mCNTs including electrical sensing which requires the integration of mCNTs into an electronic circuit. Biosensors can offer a fast and cost-effective method for bacteria detection, which can be performed on site without the need of a specialized user. The goal in this project is to develop a chemiresistive mCNT sensor which can detect the presence of bacteria at the site.

For a bacteria sensor, the main parameters are almost the same as mentioned earlier. Differences exist in the areas where sensors are being used. In general sensors are preferred to be small in size, easy to operate which does not require complicated sample preparation process, inexpensive, and label free.

For ideal sensors, design and fabrication should be in such a way that operate at the site of interest and work with complex matrices such as blood, food, water and beverage samples.

Also, samples are label free with sensitivity less than  $10^3$  CFU/mL and should distinguish between different serotypes of bacteria such as *E. coli* K12 and *Bacillus subtilis* within 5 to 10 minutes. In terms of skill, optimum condition is to be developed so that sensor requires no specialist training to perform the test. Finally, biorecognition elements must be stable at high temperatures for good shelf life.

Different methods of identifying and quantifying bacteria include 1) microbial culture, 2) metabolic activity measurements, 3) immunoassays, 4) nucleic acid assays, and 5) microscopic and other optical or imaging methods. Currently, the identification and quantification of bacteria is done extensively using microbial culture under controlled laboratory conditions, where bacteria grow and form colonies. The number of colonies observed under a microscope is an indication of the number of bacteria present in the original sample that were capable of forming colonies. The method of microbial culture requires sample preparation, concentration, purification, separation, reagents, long incubation times and controlled laboratory environments [136]. This colony forming unit (CFU) characterization has become the standard for decision making in various water sectors. Although, real-time PCR has revolutionized the detection of microorganisms in clinical laboratories [137], the technique is expensive and requires trained personnel. Microscopic methods to detect bacteria include laser-based flow cytometry and fluorescent cell sorting. Both methods are relatively expensive and require special equipment to run processes [138,139]. Multiple immunoassay based tests have been developed for bacterial detection, e.g., conjugation of fluorescent antibodies with antigens present on the surface of the bacteria for direct or indirect immunofluorescence [140,141]. There is an ongoing

effort to develop portable sensors, that could detect *E. coli* and other pathogens [142-147]. Different techniques have been reported for detection of *E. coli*. Optical, electrical and electrochemical sensors [148-152] provide good limit of detection (LOD).

Carbon nanotube-based sensors have been an area of significant interest due to their excellent physical, electrical and chemical properties of CNTs. In contrast to single walled CNTs (SWCNTs), multiwalled CNTs (MWCNTs) are chemically more stable and synthesized at lower cost while also providing multiple functionalization opportunities. Electrical response of SWCNTs to specific biological species has led to resistance and field effect transistor (FET) based sensors [153]. In SWCNTs based sensors, the sensing mechanism has been reported to be the modulation of Schottky barrier formed at the junction of SWCNTs and a conductive material [154]. A biosensor for the detection of *E. coli* was reported using an aptamer functionalized SWCNTs biosensor in which 2 out of 3 chips gave a positive response at a concentration of  $10^4$  CFU/mL of *E. coli* [153]. Recently, a simpler method involving drop casting or SWCNTs suspension with or without dielectrophoresis on prefabricated microelectrodes was also demonstrated allowing wider use of SWCNTs-based FET platform [155-157]. However, these sensors face a challenge of complicated, elaborate and expensive fabrication techniques that limits the scalability and thus commercialization of such sensors.

In this work, we have prepared a bio-ink with MWCNTs functionalized with magnetic nanoparticles. The sensitivity and selectivity of the chemiresistive sensor printed using bio-ink towards *E. coli* K12 (EC), is studied with *Bacillus Subtilis* (BS) as the negative control. This method allows facile printing, uses off-the-shelf antibodies and does not require

expensive clean room for fabrication. The printed sensing strips have been characterized for confirming the presence of antibody on the magnetized carbon nanotubes (mCNTs), confirming the ohmic behavior of the strip, size variation and electrical resistance.

### 4.3 Bacteria detection

In this section, the need for rapid detection of bacteria is being explained. In this study, mCNTs printed strips are conjugated with EDC/NHS followed by *E. coli* K-12 antibody. Strips are formed out of mCNT bio-ink which have been incubated for half an hour with Tween20 acting as surfactant. Surface modification in mCNTs biosensors is used to decrease non-specific binding of the various molecules to the transducing component. In this work, *E. coli* K-12 antibody is immobilized to the surface. Tween20 is dispersed onto the mCNT suspension protecting the surface against non-specific binding of analyte to receptor molecules. Electric measurement conducted on the prepared printed strips and the change in current with respect to change in time is studied and reported below.

#### 4.3.1 Introduction to bacteria

*Escherichia coli* (*E. coli*), refers to a large group of bacteria that is generally found in the intestines of humans and animals, mostly due to consumption of contaminated food or water. In general, almost all the strains of *E. coli* are harmless, however certain strains such as *E. coli* O157:H7 cause harmful diseases even leading to death.

Water and food borne pathogens monitoring is one of the most important issues to the health and wellbeing of the societies. There will be many advantages for industries as well



as individuals by developing a rapid bacteria detection sensor capable of detecting water and foodborne pathogens at the lowest limit of detection. Being able to determine the contamination in water sources, people in developing countries can avoid diseases such as ingesting diarrhea caused by *E. Coli*.

*E. coli* bacteria are rod-shaped cells and typically about 2.0  $\mu\text{m}$  long and 0.25  $\mu\text{m}$  to 1.0  $\mu\text{m}$  in diameter, with a cell volume of 0.6-0.7 $\mu\text{m}^3$  [13]. Cells can grow and culture easily in laboratories. Optimum growth conditions are temperature of 37°C and in a laboratory media such as lysogeny broth (LB broth).

Because of being the host organisms for majority of the work with DNA and its rapid growth rate in fresh fecal matter, *E. coli* has become the most interesting model organism for biotechnology studies. The reason for using the *E. coli* K-12, as target bacteria in this study, is being well-adapted and also, a cultivated strain in the laboratory environment [16].

Unlike other serotypes, K-12, is known to protect wild-type strains from antibodies and other chemical attacks. Because of this, in 1997, the entire genome of K-12 was sequenced.

Based on huge number of investigations on K-12, many research groups have used K-12 for evolutionary experiments. Nowadays, point-of-care devices are limited to use in clinics because of their sample volume requirements. Household devices can also allow people monitor their intake of samples which may contain bacteria and determine the chance of growing diseases. This will help to decrease the probability of bacteria caused illnesses significantly. Preventing bacteria from growing and therefore decrease the chance of diseases not only save many lives, but also save money and time from individuals filling up the ER. Rapid detection of bacteria using mCNTs biosensors can increase significantly

by increasing the sensitivity and specificity of the device. The characteristics of this biosensor which makes it cheap and easy to use are valuable potentials for the sensor to applied in the field of bacteria detection.

#### *4.3.2 Fabrication method*

The goal of this project is to develop a label free mCNTs based sensor capable of detecting bacteria. In order to achieve bacteria sensing, EDC/NHS is added to the mCNTs surface as a linker to help *E. coli* K12 antibodies immobilize to the surface of mCNTs. Tween20 is also added to the suspension for blocking the surface of mCNTs and eliminate non-specific binding. The method used to immobilize the antibodies to the surface of the mCNTs is discussed in chapter 2. Antibodies conjugate to the surface of the mCNTs by covalent binding in an overnight incubation. Before antibody immobilization, blocking agent Tween 20 is dispersed on the surface of mCNTs for half an hour. This process ensures that only specific binding occurs between receptor and analyte molecules on the surface of the mCNTs and also help to prepare a uniform printed strip. After the three steps, the substrate is prepared and ready for bacteria immobilization.

### 4.4 Results and discussions

#### *4.4.1 Visualization of bacteria*

Visualizing bacteria using optical microscope was performed to count the number of cells in 1 ml of each bacteria concentrations that is measured via OD measurement. Figure 4.1 shows the micrographs of different concentrations which are from 5  $\mu$ l of each sample. The number of bacteria in each graph is counted using ImageJ. By calculating the volume of each window again using ImageJ, the number of bacteria per volume in each graph can be

determined. The area of cover slip is  $4.8 \times 10^2 \text{ mm}^2$  and 5 ul of sample is spiked among two cover slips and placed under the microscope. Based on this volume and area of cover slip, the height is  $10.4 \text{ }\mu\text{m}$ . Area of each window calculated using ImageJ is  $2.9 \times 10^{-3} \text{ mm}^2$ . Therefore, the volume of each image is  $3.01 \times 10^{-7} \text{ ml}$ . The ratio between the volume of cover slip and volume of each window is called volume factor. In this case the number measured for volume factor is  $1.6 \times 10^3$ . Number of bacteria per volume in each graph multiple by the volume factor provide us with an approximate estimation of bacteria for each concentration in 5 ul of the sample. According to table 4.1, It can be seen that the results obtained by OD measurements for one milliliter of the solution are similar to optical microscopy.

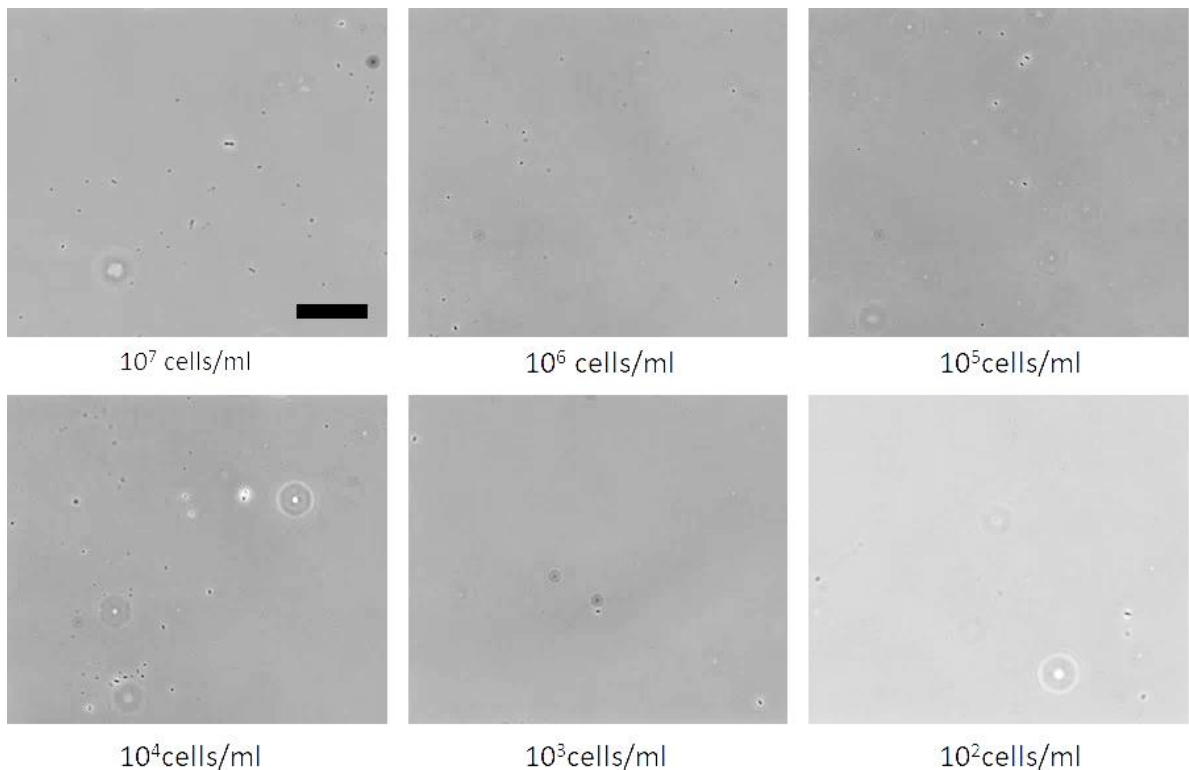


Figure 4.1: Optical microscopy images for different concentration of bacteria. Scale bar is  $50 \text{ }\mu\text{m}$ .

Table 4.1 Number of bacteria calculated in each concentration of bacteria by optical microscope versus optical density measurement

<b><i>E. coli</i> concentration (cells/ml)</b>	$10^7$	$10^6$	$10^5$	$10^4$	$10^3$	$10^2$
<b><i>E. coli</i> count in each graph</b>	40	10	5	3	----	---
<b><i>E. coli</i> count in 5 <math>\mu</math>l</b>	$6.4 \times 10^4$	$1.6 \times 10^4$	$8 \times 10^3$	$4.8 \times 10^3$	----	---
<b><i>E. coli</i> count in 1 ml</b>	$1.2 \times 10^7$	$3.2 \times 10^6$	$1.6 \times 10^6$	$9.6 \times 10^5$	----	----

According to this method, we are assuming that the bacteria cells are spreading uniformly all around the cover slip and also the 1 ml tube. But in experiment this will not happen and after concentration of  $10^5$ , the bacteria are extremely non-uniform. Therefore, the error for the concentrations below  $10^5$ , is very low. In this case we should consider that the whole number of bacteria is the same as number of bacteria we can count in each graph.

#### 4.4.2 *E. coli* K12 sensing

Fresh samples of BS and EC are prepared within inoculated tubes containing 6 mL of LB media and cultured overnight at 37°C with continuous agitation in a shaking incubator. The cultured bacteria samples are washed trice with 1x PBS and finally resuspended in 1.5 mL of 1x PBS to prepare the stock solution. Bacteria concentrations in these stock solutions are measured using a spectrophotometer by measuring the optical density at 600nm ( $OD_{600}$ ). Serial dilutions of the bacteria samples were prepared in DI water.

For electrical measurement, the flow cell is placed at the centre of the glass slide with the printed sensing strip. Alligator clips with flat ends are attached to the exposed sensing strip

on either side of the flow cell. A microcontroller board (Arduino Uno) is used to supply a voltage of 5V across the electrical circuit, the details of which is provided in our previous work [31]. An external resistance of 1 M $\Omega$  is placed in series with the sensing strip. The built-in analog to digital converter measures the feedback voltage drop across the sensing strip. The sampling frequency is 10 Hz and the current through the sensing strip is calculated from the measured voltage drop. Electrical measurements were performed for 120s after the bacteria sample is injected into the flow cell and the responses are normalized to the dry sensor current before addition of the sample.

#### *4.4.2.1 Detection of E. coli whole cell*

The working principle of the sensor is the specific binding of the antibody functionalized over the surface of mCNTs with the surface antigens present on the bacterial cell wall. The different performance metrics of the sensor such as sensitivity, selectivity and response time for the detection of *E. coli* K12 bacteria is investigated. The initial investigation is focused on determining the time dependent response of the biosensor to establish the required incubation time for maximum sensor response. 4  $\mu$ L of the bacteria sample with highest concentration of  $10^7$  cells/ml is dispensed within the flow cell (shown in figure 3.2) at room temperature and the biosensor response is measured. As the surface antigens present on the bacterial cell wall binds to the primary antibody on mCNTs, the resistance of the strip increases and the current across the strip decreases. The decrease in normalized current,  $I/I_0$  ( $I$  is the instantaneous current of the biosensor after exposure to bacteria sample and  $I_0$  is the initial biosensor current, after functionalization), as a function of time is

recorded. As evident in figure. 4.2b, the biosensor response can be obtained in 2 minutes and sensitivity of different concentrations of bacteria is detectable in less than two minutes.

Biosensor sensitivity was studied by measuring the decrease in current. Figure 4.2 shows the results of decrease in current for different concentrations of bacteria. 7.14 $\mu$ g of *E. coli* K12 polyclonal antibody is used for each 1 mg of mCNTs for immobilization and 4 $\mu$ L of the respective bacteria sample is injected to the flow cell over the biosensor. The results show that after 120 seconds, it is possible to distinguish between different concentrations of the *E. coli* K12 bacteria.

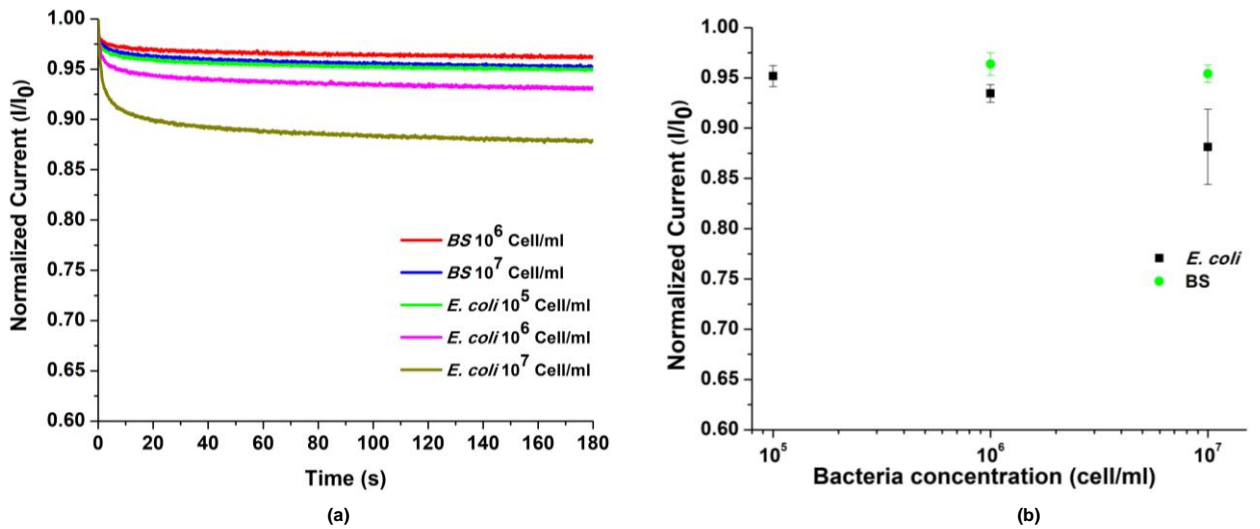


Figure 4.2: Performance of the biosensor with sample containing whole bacterial cell. (a) Average of the normalized current with time for different bacterial concentrations and (b) the normalized current response at  $t = 120$ s with standard deviations. Number of samples,  $n \geq 4$ .

Gram-negative bacteria such as *E. coli* have an overall negative charge over the external membrane in the lipopolysaccharide, where the O antigen resides. Their attachment onto mCNTs is expected to cause an increase in the resistance on p-type SWCNTs in the Debye

length where the biosensor is sensitive [32]. Because these bacteria have a size of around  $0.8\mu\text{m}\times 1.5\mu\text{m}$ , it is expected that only the charges in the Debye length will produce some effect in the biosensor.

In order to check the reproducibility of the biosensor, same experiment was performed using the same protocol for making the biosensor and detecting bacteria. Results matches with the previous data which indicates that the biosensor has reproducibility (Figure 4.3).

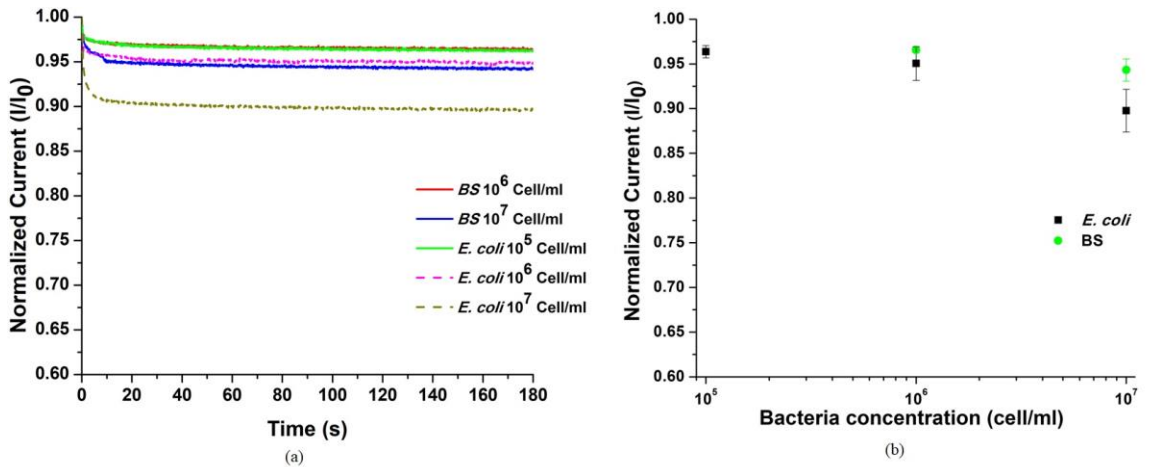


Figure 4.3. Performance of the biosensor with sample containing whole bacterial cell. (a) Average of the normalized current with time for different bacterial concentrations and (b) the normalized current response at  $t = 120\text{s}$  with standard deviations. Number of samples,  $n \geq 4$ .

#### 4.4.2.1 Detection of *E. coli* with cell lysates

In an attempt to improve the limit of detection of the biosensor, detection of lysed cells is investigated. In this experiment, commercially available cell lysis buffer, BugBuster is used to lyse the bacteria cell and the response is compared to non-lysed cell. As evident from figure 4.4 use of lysed cells improved the limit of detection to a concentration of  $10^3$  cells/mL. In order to lyse the cells, serial dilutions of both EC and BS made out of highest

concentration to  $10^2$  cells/mL in 1.5 mL tube. 50  $\mu\text{g/mL}$  of BugBuster was added to each dilution and incubated at room temperature for 30 minutes.

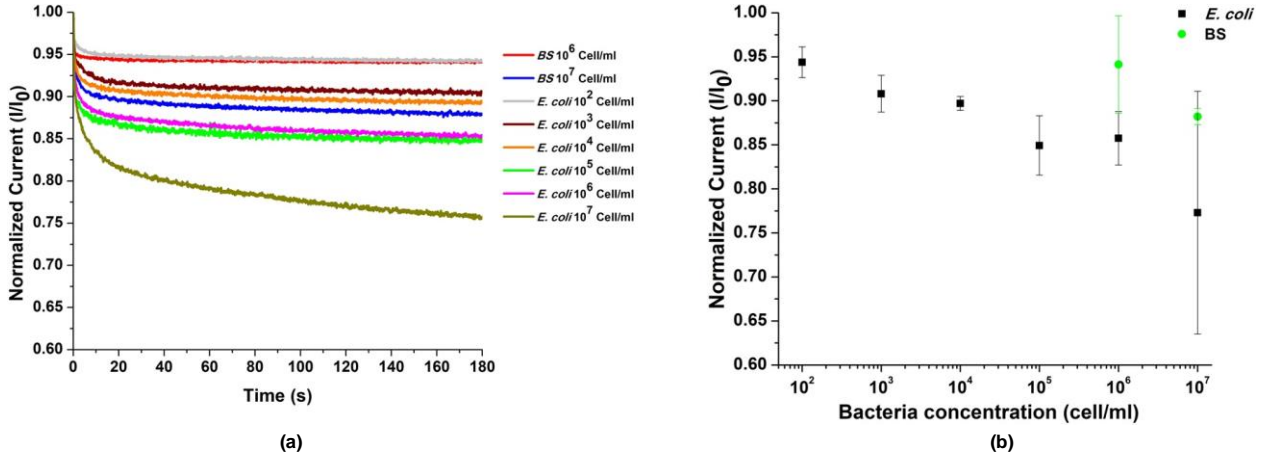


Figure 4.4. Performance of the biosensor with sample containing bacterial cell lysate. (a) The average variation of the normalized current with time for different bacterial concentrations and (b) the normalized current response at  $t = 120$ s with standard deviations. Number of samples,  $n \geq 4$ .

The possible reason for improved sensitivity with cell lysates could be more accessibility of the surface antigens present on the cell wall of *E. coli* K12. Additionally, another advantage of lysing the cells for detection is significant decrease in standard deviation. This will also be attributed to the particle size and higher diffusivity of surface antigens to the Abs.

Considering the control, a smaller response was measured for the same concentrations of lysed B.S cells, which confirms the better selectivity of the sensor.



## 5. Summary and Future Work

### 5.1 Conclusion

To summarize, a sensitive and selective mCNTs-based chemiresistive sensors have been developed for detecting *E. coli* K12 using a simple and affordable method that can be applied in most laboratories and on-site. A limit of detection of  $10^5$  cells/mL is achieved for detection of *E. coli* K12. In the case of cell lysate, limit of detection reaches to  $10^2$  cells/mL. Although lower limit of detection has been reported for bacteria using other techniques, the advantages of this sensor rely on its simple measurement performance, allowing measurements to be performed almost in a real-time manner at room temperature. The integration of nanostructures such as mCNTs into microelectronic devices in combination with the use of specific recognition molecules such as Abs has shown promising results for the next generation of truly miniaturized, sensitive, and cost-effective sensors. Since the sensing area of the device is of few millimeters in size, recirculation of the sample may increase the chance for a single particle to reach this area.

### 5.2 Future Work

Future work is required for the results seen in section 4.4.2. This is because the results shown in this section do not contain a higher limit of detection. With a further understanding of what happens on the surface of the CNT when bacteria is introduced, optimization of the CNT test strip can lead to a lower limit of detection. A further

understanding of the current response to bacteria and negative control is also required. Studies indicate that the drop in current should change with respect to concentration of bacteria. However, this was not the case for all the concentrations that were tested. The resistance for bacteria sensing below  $10^5$  cells/mL also did not have the expected pattern. Although there was a successful response from the devices to the antibody immobilization followed by the  $10^5$  cells/mL, a further study on this concentration would provide a better understanding as to why there was no observed change in the current there from the DI water and BS bacteria. These results did show a good understanding to the change in resistance with respect to literature review but there is no clear understanding as to what goes on with the interaction between bacteria and CNTs. Future work should also involve another method of determining what is happening on the surface of the CNTs when they undergo surface immobilization with bacteria. Fluorescent visualization and atomic force microscopy would be ideal where counting the bacteria cells that binds to the surface of the CNTs can confirm whether or not the electrical response is in fact coming from the antibody to bacteria binding and not somewhere else.

### 5.3 Summary

The main goal of this research was to study the potential of using CNTs as chemiresistive biosensors and to develop a label free, real-time point of care biosensor capable of detecting bacteria. In order to accomplish the goal, successful fabrication and characterization of the device was required. We attempted to detect *E.coli* K-12 sensing abilities and underlying sensing mechanism, as well as commercialization of the CNTs chemiresistive biosensor. Results from fluorescent microscopy successfully proved that Abs are conjugated to the

surface of CNTs and is a reason in order to confirm the underlying sensing mechanism. By using EDC/NHS as a crosslinker to attach Abs to the carboxylic groups present on the surface of CNTs, we can provide a platform for binding between Abs and antigen. Immobilizing Abs with CNTs confirmed that with an increase in the concentration of Ab, specific binding between bacteria and Abs is stronger therefore, resistance of the biosensor also increases.

Detection of  $10^5$  cells/mL of *E.coli* K-12 was also accomplished using the developed biosensors. In the case of lysate bacteria the higher sensitivity could be obtained and we were able to detect  $10^2$  cells/mL. Impedance studies for biosensing applications have proven to be a very good tool in determining the effects of surface charge electrochemically. Impedance techniques were able to determine changes occurring on the surface of the CNT almost immediately via electrochemically. These results proved that the sensitivity of the CNT biosensor that can be used for the detection of bacteria lower than  $10^5$  cells/mL and therefore allowing for a successful fabrication of a portable CNT device that is in real-time, point of care.

## 6. References

1. Bhalla, N. *et al.* Introduction to biosensor. *Essays biochem.* **60**, 1-8 (2016).
2. Murugaiyan, B. S. *et al.* Biosensors in clinical chemistry: An overview. *Advanced Biomed Research*, **3**, 67, (2014).
3. Thevenot, D. *et al.* Electrochemical biosensors: Recommended definitions and classification. *Pure and applied chemistry.* **71**, 2339-2348 (2009).
4. Veetil, J. V & Ye, K. Development of Immunosensors Using Carbon Nanotubes. *Biotechnol. Prog.* **23**, 517-531 (2007).
5. Joseph, W., Carbon nanotube based electrochemical biosensor. *Analytical Chem.* **17**, 7- 14 (2005).
6. Dantham, V. R. *et al.* Label-Free Detection of Single Protein Using a Nanoplasmonic- Photonic Hybrid Microcavity. *Nano Lett.* **13**, 3347–3351 (2013).
7. He, L., Ozdemir, S. K., Zhu, J., Kim, W. & Yang, L. Detecting single viruses and nanoparticles using whispering gallery microlasers. *Nat. Nanotechnol.* **6**, 428–32 (2011).
8. Vollmer, F., Arnold, S. & Keng, D. Single virus detection from the reactive shift of a whispering-gallery mode. *Proc. Natl. Acad. Sci. U. S. A.* **105**, 20701–20704 (2008)
9. Washburn, A. L., Luchansky, M. S., Bowman, A. L. & Bailey, R. C. Quantitative, Label Free Detection of Five Protein Biomarkers Using Multiplexed Arrays of Silicon Photonic Microring Resonators. *Anal. Chem.* **82**, 69–72 (2010)
10. Zhu, H., White, I. M., Suter, J. D., Zourob, M. & Fan, X. Opto-fluidic micro-ring resonator for sensitive label-free viral detection. *Analyst* **133**, 356–360 (2008).
11. Huang, M. J. *et al.* Serotype-Specific Identification of Dengue Virus by Silicon Nanowire Array Biosensor. *J. Nanosci. Nanotechnol.* **13**, 3810–3817 (2013).
12. Huang, Y.W. *et al.* Real-Time and Label-Free Detection of the Prostate-Specific Antigen in Human Serum by a Polycrystalline Silicon Nanowire Field-Effect Transistor Biosensor. *Anal. Chem.* **85**, 7912–7918 (2013).
13. Patolsky, F. *et al.* Electrical detection of single viruses. *Proc. Natl. Acad. Sci. U. S. A.* **101**, 14017–22 (2004).
14. Shirale, D. J. *et al.* Label-free chemiresistive immunosensors for viruses. *Environ. Sci. Technol.* **44**, 9030–5 (2010).
15. Tuan, C. Van, Huy, T. Q., Hieu, N. Van, Tuan, M. A. & Trung, T. Polyaniline Nanowires- Based Electrochemical Immunosensor for Label Free Detection of Japanese Encephalitis Virus. *Anal. Lett.* **46**, 1229–1240 (2013).
16. Vidic, J. *et al.* Surface Plasmon Resonance Immunosensor for Detection of PB1-F2 Influenza A Virus Protein in Infected Biological Samples. *J. Anal. Bioanal. Tech.* **S7**, 1–7 (2013).
17. Wang, S. *et al.* Label-free imaging, detection, and mass measurement of single viruses by surface plasmon resonance. *Proc. Natl. Acad. Sci. U. S. A.* **107**, 16028–32 (2010).
18. Yakes, B. J. *et al.* Surface plasmon resonance biosensor for detection of felin calicivirus, a surrogate for norovirus. *Int. J. Food Microbiol.* **162**, 152-158 (2013).

19. Lazcka, O., Javier Del Campo, F., Xavier Munoz, F., Pathogen detection: A perspective of traditional methods and biosensors. *Biosen. and Bioelec.* **22**, 1205-1217 (2007)
20. Malhotra, Sh. *et al.* Biosensors: Principle, types and applications. *IJARIE*. 3, 2395-4396 (2017).
21. Monk, J, Walt R. Optical-fiber based biosensors. *Analytical and bioanalytical chemistry*. 397, 931-945 (2004).
23. .Korotkaya, E.V. Biosensors, design, classification, and applications in the food industry. *Foods and Raw materials*. 2, 2308-4057 (2014).
24. Bergveld, P. Development of an ion-sensitive solid-state device for neurophysiological measurements. *IEEE Trans. Biomed. Eng.* **BME-17**, 70-71 (2013).
25. Ward, A., A study of mechanisms governing single walled carbon nanotube thin film electric biosensors. *Unpublished master's thesis*, 4-6 (2013).
26. Luo, X. & Davis, J. J. Electrical biosensors and the label free detection of protein disease biomarkers. *Chem. Soc. Rev.* **42**, 5944–62 (2013).
27. Kurkina, T., Label-free electrical biosensing based on electrochemically functionalized carbon nanostructures. *Thesis dissertation*, 14-17 (2012).
28. Yang, W., Ratinac, K. R., Ringer, S. P., Thordarson, P., Gooding, J., Braet, F. Carbon Nanomaterials in Biosensors: Should you use nanotubes or graphene? *Angew. Chem. Int. Ed.* **49**, 2114-2138 (2010).
29. Nair, P. R. & Alam, M.A. Screening-limited response of nanobiosensors. *Nano Lett.* **8**, 1281-1285 (2008).
30. Nair, P. R. & Alam, M. A. Dimensionally Frustrated Diffusion towards Fractal Adsorbers. *Phys. Rev. Lett.* **99**, 256101 (2007).
31. Lee, K., Nair, P. R., Scott, A., Alam, M. a. & Janes, D. B. Device considerations for development of conductance-based biosensors. *J. Appl. Phys.* **105**, 102046 (2009).
32. Kocabas, C., Shim, M., Rogers, J.A., Spatially selective guided growth of high-coverage arrays and random networks of single-walled carbon nanotubes and their integration into electronic devices. *J. Am. Chem. Soc.* **128**, 4540-4541 (2006).
33. Jacobs, C., Peairs, M., Venton, B., Review: carbon nanotube based electrochemical sensors for biomolecules. *Anal. Chem. Acta* **662**, 105-127 (2010).
34. Nair, P. R., Alam, M. A. Performance limits of Nanobiosensors. *Apps. Phys. Lett.* **88**, 9 11 (2006).
35. Garcia-Aljaro, C., Cella, L., Shirale, D., Park, M., Munoz, FJ., Yates, MV., Mulchandani, A. Carbon nanotubes-based chemiresistive biosensors for detection of microorganisms. *Biosens. Bioelectron.* **26**(4), 1437-41 (2010).
36. Dong, B. X. *et al.* Electrical Detection of Femtomolar DNA via Gold-Nanoparticle Enhancement in Carbon-Nanotube-Network Field-Effect Transistors. *Adv. Mater.* **20**, 2389–2393 (2008).
37. Lee, D., Chander, Y., Goyal, S. M. & Cui, T. Carbon nanotube electric immunoassay for the detection of swine influenza virus H1N1. *Biosens. Bioelectron.* **26**, 3482–7 (2011).

38. Schoning, M., Poghossian, A. Recent advances in biologically sensitive field effect transistors. *Anal.* **127**, 1137-1151 (2002).
39. Thomas, M.K., Murray, R., Flockhart, L., Pintar, K., Fazil, A., Nesbitt, A., Marshall, B., Tataryn, J., Pollari, F. Estimates of foodborne illness-related hospitalizations and deaths in Canada for 30 specified pathogens and unspecified agents. *Foodborne Pathog. Dis.* **12**, 820-827 (2015).
40. Chaib, F., WHO's first ever global estimates of foodborne diseases find children under 5 account for almost one third of deaths. [www.who.int/foodborne-disease-estimates](http://www.who.int/foodborne-disease-estimates). *World Health Org.* (2015).
41. Ahmed, A., Rushworth, J., Hirst, N. Biosensors for Whole-Cell Bacterial Detection. *Clin Microbiol Rev.* **27**, 631-646 (2014).
42. Aqui, L., Yanez-Sedeno, P., Pingarron, J. Role of carbon nanotubes in electroanalytical chemistry: a review. *Anal Chem Acta.* **622**, 11-47 (2008).
43. Pumera, M., Sanchez, S., Ichinose, I., Tanj, J. Electrochemical nanobiosensors. *Sens. And Act.* **123**, (2007).
44. Rao, C., Satishkumar, B., Govindaraj, A., Nath, M. Nanotubes. *Chem. Phys. Chem.* **2**, 78 -105 (2001).
45. Ward, A., Petrie, A., Honek, J., Tang, X., Analyte dependent sensing mechanisms governing single walled carbon nanotube thin film biosensors. *IEEE Nano. Tech. Mag.* **8**, 29 -37 (2014).
46. Novoselov, K., Geim, A., Morosov, S., Jiang, D., Zhang, Y., Dubonos, S., Grigorieva, I., Firsov, A. Electric Field effect in atomically thin carbon films. *Sci.* **306**, 666-9 (2014).
47. Ajayan, P., Nanotubes of Carbon. *Chem. Rev.* **99**, 1787-99 (1999).
48. Torres, L., Roche, S., Charlier, J.C. Introduction to Graphene-Based Nanomaterials: From Electronic Structure to Quantum Transport. *Contem. Phys.* **4**, 344-45 (2014).
49. Jariwala, Z., Sangwan, K., Lauhon, L., Marksab, T., Hersam, M. Carbon nanomaterials for electronics, optoelectronics, photovoltaics, and sensing. *Chem. Soc. Rev.* **42**, 2824 (2013).
50. Iijima, S. and T. Ichihashi, Single-shell carbon nanotubes of 1-nm diameter. *Nature*, **363**: p. 603-605 (1993).
51. Bethune, D., *et al.*, Cobalt-catalysed growth of carbon nanotubes with single-atomic-layer walls. *Nature*, **363**: p. 505-507 (1993).
52. Wernik, J.M. and S.A. Meguid, Recent developments in multifunctional nanocomposites using carbon nanotubes. *Applied Mechanics Reviews*, **63**(5): p. 050801 (2010).
53. Varshney, K., Carbon nanotubes: a review on synthesis, properties and applications. *International Journal of Engineering Research*, **2**(4): p. 660-677, (2014).
54. Britz, D. and Khlobystov, A., Noncovalent interactions of molecules with single walled carbon nanotubes. *Chem. Soc. Rev.* **35**, 637-659 (2006).
55. Jorio, A., G. Dresselhaus, and M.S. Dresselhaus, Carbon nanotubes: Advanced topics in the synthesis, structure, properties and applications. *Topics in applied physics*: Springer. (2008).

56. Yu, X., Munge, B., Patel, V., Jensen, G., Bhirde, A., Gong, J.D., Kim, S.N., Gillespie, J., Gutkind, J.S., Papadimitrakopoulos, F. and Rusling, J.F. Carbon nanotube amplification strategies for highly sensitive immunodetection of cancer biomarkers. *J. Am. Chem. Soc.* **128**, 11199-11205 (2006).
57. Heller, I., Kong, J., Heering, H., Williams, K.A., Lemay, S.G., Dekker, C. Individual singlewalled carbon nanotubes as nanoelectrodes for electrochemistry. *Nano Lett.* **5**, 137- 142, (2005).
58. Saito, R., G. Dresselhaus, and M.S. Dresselhaus, Physical properties of carbon nanotubes. *World Scientific*, 35. (1998).
59. De Volder, M.F., *et al.*, Carbon nanotubes: present and future commercial applications. *Science*. **339**(6119): p. 535-539, (2013).
60. Sinha, N., J. Ma, and J.T. Yeow, Carbon nanotube-based sensors. *Journal of Nanoscience and Nanotechnology*, **6**(3): p. 573-590. (2006).
61. Mahar, B., *et al.*, Development of carbon nanotube-based sensors—a review. *Sensors Journal, IEEE*. **7**(2): p. 266-284. (2007).
62. Peng, L.-M., Z. Zhang, and S. Wang, Carbon nanotube electronics: recent advances. *Materials Today*, **17**(9): p. 433-442. (2017).
63. Szabó, A., *et al.*, Synthesis methods of carbon nanotubes and related materials. *Materials*, **3**(5): p. 3092-3140. (2010).
64. Park, S., *et al.*, Carbon nanosyringe array as a platform for intracellular delivery. *Nano Letters*, **9**(4): p. 1325-1329. (2009).
65. Sinha, N. and J.T. Yeow, Carbon nanotubes for biomedical applications. *NanoBioscience, IEEE Transactions on*, **4**(2): p. 180-195. (2005).
66. Zhu, Y., C. Xu, and L. Wang, Carbon nanotubes in biomedicine and biosensing: *INTECH Open Access Publisher*. (2011).
67. Shao, W., *et al.*, Carbon nanotubes for use in medicine: Potentials and limitations. *Syntheses and Applications of Carbon Nanotubes and Their Composites. Croatia: InTech*, p. 285-311. (2013).
68. Antiohos, D., *et al.*, Carbon nanotubes for energy applications. *Syntheses and Applications of Carbon Nanotubes and Their Composites*, p. 496-534. (2013).
69. Dhavle, J., Carbon nanotubes' use in energy storage. *Storage4*, (2013).
70. Popov, V.N. and P. Lambin, Carbon nanotubes: from basic research to nanotechnology. 222. *Springer Science & Business Media*. (2006).
71. Huang, J. Atomic structure and electronic properties of single-walled carbon nanotubes. *Nat.* **391**, 1997-99 (1998).
72. Skulason, E. Metallic and Semiconducting properties of Carbon Nanotubes. *Mod. Phys.* **2**, 8-21 (2005).
73. Minot, E. Tuning the band structure of carbon nanotubes. *Ph.d Thesis*, 15-21, (2004).
74. Krapf, D., Quinn, B., Wu, M.-Y., Zandbergen, H.W., Dekker, C., Lemay, S.G. Experimental observation of nonlinear ionic transport at the nanometer scale. *Nano Lett.*, **6**, 2531-35 (2006).

75. Gooding, J., Chou, A., Liu, J., Losic, D., Shapter, J., Hibbert, D. The effects of the lengths and orientations of single-walled carbon nanotubes on the electrochemistry of nanotube-modified electrodes. *Electro. Comm.*, **9**, 1677-1683 (2007).
76. Guiseppi-Elie, A., Lei, C., Baughman, R. Direct electron transfer of glucose oxidase on carbon nanotubes. *Nanotech.*, **13**, 559 (2002).
77. Chen, Z., Tabakman, S.M., Goodwin, A.P., Kattah, M.G., Daranciang, D., Wang, X., Zhang, G., Li, X., Liu, Z., Utz, P.J., Jiang, K., Fan, S. and Dai, H. Protein microarrays with carbon nanotubes as multicolor Raman labels. *Nat. Biotechnol.* **26**, 1285-1292 (2008).
78. Alwarappan, S., Erdem, A., Liu, C., Li, C.Z. Probing the electrochemical properties of graphene nanosheets for biosensing applications. *J. Phys. Chem.* **113**, 8853-57 (2009).
79. Yu, X., Munge, B., Patel, V., Jensen, G., Bhirde, A., Gong, J.D., Kim, S.N., Gillespie, J., Gutkind, J.S., Papadimitrakopoulos, F. and Rusling, J.F. Carbon nanotube amplification strategies for highly sensitive immunodetection of cancer biomarkers. *J. Am. Chem. Soc.* **128**, 11199-11205 (2006).
80. Balasubramanian, K., Burghard, M. Biosensors based on carbon nanotubes. *Anal. Bioanal. Chem.* **385**, 452-468 (2006).
81. Sotiropoulou, S., Chaniotakis, N.A., Carbon nanotube array-based biosensor. *Anal Bioanal. Chem.* **375**, 103-105 (2003).
82. Yu, X., Chattopadhyay, D., Galeska, I., Papadimitrakopoulos, F., Rusling, J.F. Peroxidase activity of enzymes bound to the ends of single-wall carbon nanotube forest electrodes. *Electrochem. Comm.* **5**, 408-411 (2003).
83. Collins, P.G., Bradley, K., Ishigami, M., Zettl, A. Extreme oxygen sensitivity of electronic properties of carbon nanotubes. *Science.* **287**, 1801-1804 (2000).
84. Besteman, K., Lee, J-O., Wiertz, F.G.M., Heering, H.A., Dekker, C. Enzyme-Coated Carbon Nanotubes as Single-Molecule Biosensors. *Nano Lett.* **3**, 727-730 (2003).
85. Star, A., Tu, E., Niemann, J., Gabriel, J-CP., Joiner, C.S., Valcke, C. Label-free detection of DNA hybridization using carbon nanotube network field-effect transistors. *Proc. Natl. Acad. Sci. USA.* **103**, 921–926 (2006).
86. Maehashi, K., Matsumoto, K., Takamura, Y., Tamiya, E. Aptamer-based label-free immunosensors using carbon nanotube field-effect transistors. *Electroanal.* **21**, 1285- 1290 (2009).
87. Gruner, G. Carbon nanotube transistors for biosensing applications. *Anal. Bioanal. Chem.* **384**, 322-335 (2006).
88. Ando, Y. and X. Zhao, Synthesis of carbon nanotubes by arc-discharge method. *New Diamond and Frontier Carbon Technology*, **16**(3): p. 123-138. (2006).
89. Rafique, M.M.A. and J. Iqbal, Production of carbon nanotubes by different routes- a review. *Journal of Encapsulation and Adsorption Sciences*, **1**(02): p. 29. (2011).
90. Prasek, J., *et al.*, Chemical Vapor Depositions for Carbon Nanotubes Synthesis. *Nova Science Publishers.* p. 87-106. (2013).



91. Terranova, M.L., V. Sessa, and M. Rossi, The world of carbon nanotubes: an overview of CVD growth methodologies. *Chemical Vapor Deposition*, **12**(6): p. 315-325. (2006).
92. O'connell, M.J., Carbon nanotubes: properties and applications. *CRC press*. (2006).
93. Charlier, J. C. Electronic and transport properties of nanotubes. *Rev. Mod. Phys.* **79**, 677- 732 (2007).
94. Choudhary, V. and A. Gupta, Polymer/carbon nanotube nanocomposites. *Carbon Nanotubes-Polymer Nanocomposites*, p. 65-90. (2011)
95. Kimura, T., *et al.*, Polymer composites of carbon nanotubes aligned by a magnetic field. *Advanced Materials*, **14**(19): p. 1380-1383. (2002).
96. Homma, Y., *et al.*, Photoluminescence measurements and molecular dynamics simulations of water adsorption on the hydrophobic surface of a carbon nanotube in water vapor. *Physical Review Letters*, **110**(15): p. 157402. (2013).
97. Fam, D. W. H., Palaniappan, A., Tok, a. I. Y., Liedberg, B. & Moochhala, S. M. A review on technological aspects influencing commercialization of carbon nanotube sensors. *Sensors Actuators B Chem.* **157**, 1–7 (2011).
98. V Ovchinnikov, A.A., Giant diamagnetism of carbon nanotubes. *Physics Letters A*, **195**(1): p. 95-96. (1994).
99. Kim, Y., *et al.*, High-purity diamagnetic single-wall carbon nanotube buckypaper. *Chemistry of Materials*, **19**(12): p. 2982-2986. (2007).
100. Ciraci, S., *et al.*, Functionalized carbon nanotubes and device applications. *Journal of Physics: Condensed Matter*, **16**(29): p. R901. (2004).
101. Atieh, M.A., Effect of functionalized carbon nanotubes with carboxylic functional group on the mechanical and thermal properties of styrene butadiene rubber. *Fullerenes, Nanotubes and Carbon Nanostructures*, **19**(7): p. 617-627. (2011).
102. Naseh, M.V., *et al.*, Functionalization of carbon nanotubes using nitric acid oxidation and DBD plasma. *World Academy of Science, Engineering and Technology*, **49**: p. 177-179. (2009).
103. Worsley, K.A., *et al.*, Functionalization and dissolution of nitric acid treated single-walled carbon nanotubes. *Journal of the American Chemical Society*, **131**(50): p. 18153-18158. (2009).
104. Ahmed, D.S., A.J. Haider, and M. Mohammad, Comparison of functionalization of multi-Walled carbon nanotubes treated by oil olive and nitric acid and their characterization. *Energy Procedia*, **36**: p. 1111-1118. (2013).
105. Tchoul, M.N., *et al.*, Effect of mild nitric acid oxidation on dispersability, size, and structure of single-walled carbon nanotubes. *Chemistry of Materials*, **19**(23): p. 5765-5772. (2007).
106. Datsyuk, V., *et al.*, Chemical oxidation of multiwalled carbon nanotubes. *Carbon*, **46**(6): p. 833-840. (2008).
107. Kanai, Y., *et al.*, Atomistic oxidation mechanism of a carbon nanotube in nitric acid. *Physical Review Letters*, **104**(6): p. 066401. (2010).
108. Martinez MT., Tseng YC., Ormategui N., Loinaz I., Eritja R., Bokor J. Label-Free DNA Biosensors Based on Functionalized Carbon Nanotube Field Effect Transistors. *Nano Letters*. **9**, 530–536 (2011).

109. Malig J., Englert JM., Hirsch A., Guldi DM. Wet Chemistry of Graphene. *Interface*, **20**, 53- 56 (2011)
110. Getzlaff, M., *Fundamentals of magnetism*. 2007: Springer Science & Business Media.
111. Akbarzadeh, A., M. Samiei, and S. Davaran, *Magnetic nanoparticles: preparation, physical properties, and applications in biomedicine*. Nanoscale Research Letters, 2012. **7**(1): p. 1-13.
112. Ghosh, S. and I.K. Puri, Soft polymer magnetic nanocomposites: microstructure patterning by magnetophoretic transport and self-assembly. *Soft Matter*, **9**(6): p. 2024-2029. (2013).
113. Ghosh, S., *et al.*, Patterning the stiffness of elastomeric nanocomposites by magnetophoretic control of cross-linking impeder distribution. *Materials*, **8**(2): p. 474-485. (2015).
114. Jagannatham, M., S. Sankaran, and H. Prathap, Electroless nickel plating of arc discharge synthesized carbon nanotubes for metal matrix composites. *Applied Surface Science*, **324**: p. 475-481. (2015).
115. Velasco-Santos, C., A. Martinez-Hernandez, and V. Castano, Carbon nanotube-polymer nanocomposites: The role of interfaces. *Composite Interfaces*, **11**(8-9): p. 567-586. (2005).
116. Goh, P., A. Ismail, and B. Ng, Directional alignment of carbon nanotubes in polymer matrices: contemporary approaches and future advances. *Composites Part A: Applied Science and Manufacturing*, **56**: p. 103-126. (2014).
117. J Mahanthesha, P., C. Srinivasa, and G. Mohankumar, Processing and characterization of carbon nanotubes decorated with pure electroless nickel and their magnetic properties. *Procedia Materials Science*, **5**: p. 883-890. (2014).
118. Liebau, M., *et al.*, Contact improvement of carbon nanotubes via electroless nickel deposition. *Applied Physics A*, **77**(6): p. 731-734. (2003).
119. Gong, J.-L., *et al.*, Removal of cationic dyes from aqueous solution using magnetic multi-wall carbon nanotube nanocomposite as adsorbent. *Journal of Hazardous Materials*, **164**(2): p. 1517-1522. (2009).
120. K Fazelirad, H., *et al.*, Preparation of magnetic multi-walled carbon nanotubes for an efficient adsorption and spectrophotometric determination of amoxicillin. *Journal of Industrial and Engineering Chemistry*, **21**: p. 889-892. (2015).
121. Tarigh, G.D. and F. Shemirani, Magnetic multi-wall carbon nanotube nanocomposite as an adsorbent for preconcentration and determination of lead (II) and manganese (II) in various matrices. *Talanta*, **115**: p. 744-750. (2013).
122. Chen, C., *et al.*, Functionalization and magnetization of carbon nanotubes using Co-60 gamma-ray irradiation. *Journal of Magnetism and Magnetic Materials*, **367**: p. 47-52. (2014).
123. Yang, F., *et al.*, Magnetic functionalised carbon nanotubes as drug vehicles for cancer lymph node metastasis treatment. *European Journal of Cancer*, **47**(12): p. 1873-1882. (2011).

124. Sarkar, D., *et al.*, Enhanced broadband microwave reflection loss of carbon nanotube ensheathed Ni–Zn–Co-ferrite magnetic nanoparticles. *Materials Letters*, **120**: p. 259-262. (2014).
125. Tans, S. J., Verschueren, A. R. M. & Dekker, C. Room-temperature transistor based on a single carbon nanotube. *Nature* **393**, 49–52 (1998).
126. Martel, R., Schmidt, T., Shea, H. R., Hertel, T. & Avouris, P. Single- and multi-wall carbon nanotube field-effect transistors. *Appl. Phys. Lett.* **73**, 2447–2449 (1998).
127. Heller, I. *et al.* Identifying the Mechanism of Biosensing with Carbon Nanotube Transistors. *Nano Lett.* **8**, 591–595 (2008).
128. Salehi-khojin, A. *et al.* On the Sensing Mechanism in Carbon Nanotube Chemiresistors. *ACS Nano* **5**, 153–158 (2011).
129. Heller, I., Janssens, A.M., M, J., Minot, E.D., Lemay, S.G., Dekker, C. Identifying the Mechanism of Biosensing with Carbon Nanotube Transistors. *Nano. Lett.* **8**, 591-595, (2007).
130. Fam, D., Palaniappan, A., Tok, I., Liedberg, B., Moochhala, S.M. A review on technological aspects influencing commercialization of carbon nanotube sensors. *Sens. Act. B.* **157**, 1- 7 (2011).
131. Artyukhin, A.B., Stadermann, M., Friddle, R.W., Stroeve, P., Bakajin, O., Noy, A., Controlled electrostatic gating of carbon nanotube FET devices. *Nano. Lett.* **6**, 2080- 2085 (2006).
132. Fischer, J.E. Chemical Doping of Single walled carbon nanotubes. *Acc. Chem. Res.* **35**, 1079-1086 (2002).
133. Zahab, A., Spina, L., Poncharal, P. & Marliere, C. Water-vapor effect on the electrical conductivity of a single-walled carbon nanotube mat. *Phys. Rev. B* **62**, 0–3 (2000).
134. Larrimore, L., Nad, S., Zhou, X., Abruna, H. & McEuen, P. L. Probing electrostatic potentials in solution with carbon nanotube transistors. *Nano Lett.* **6**, 1329–1333 (2006).
135. Li, X., Guard, L. New doping method improves electronic properties of carbon nanotubes. (2016).
136. Lagier, J.-C., *et al.*, Current and past strategies for bacterial culture in clinical microbiology. *Clinical microbiology reviews*, **28**(1): p. 208-236. (2015).
137. Espy, M., *et al.*, Real-time PCR in clinical microbiology: applications for routine laboratory testing. *Clinical microbiology reviews*, **19**(1): p. 165-256. (2006).
138. McHugh, I.O. and A.L. Tucker, Flow cytometry for the rapid detection of bacteria in cell culture production medium. *Cytometry Part A*, **71**(12): p. 1019-1026. (2007).
139. Karo, O., *et al.*, Bacteria detection by flow cytometry, in *Clinical Chemistry and Laboratory Medicine*. p. 947. (2008).
140. Janse, J.D. and B. Kokoskova, Indirect immunofluorescence microscopy for the detection and identification of plant pathogenic bacteria (in particular for *Ralstonia solanacearum*), in *Plant Pathology*. Springer. p. 89-99. (2009)

141. Kourkine, I.V., *et al.*, Detection of Escherichia coli O157: H7 bacteria by a combination of immunofluorescent staining and capillary electrophoresis. *Electrophoresis*, **24**(4): p. 655-661. (2003).
142. Xu, M., R. Wang, and Y. Li, *Electrochemical biosensors for rapid detection of Escherichia coli O157: H7*. *talanta*, **162**: p. 511-522. (2017).
143. Dharmasiri, U., *et al.*, Enrichment and detection of Escherichia coli O157: H7 from water samples using an antibody modified microfluidic chip. *Analytical chemistry*, **82**(7): p. 2844-2849. (2010).
144. Yang, H., *et al.*, Detection of escherichia coli with a label-free impedimetric biosensor based on lectin functionalized mixed self-assembled monolayer. *Sensors and Actuators B: Chemical*, **229**: p. 297-304. (2016).
145. Tawil, N., *et al.*, Surface plasmon resonance detection of E. coli and methicillin-resistant S. aureus using bacteriophages. *Biosensors and Bioelectronics*, **37**(1): p. 24-29. (2012).
146. Bej, A.K., *et al.*, Detection of Escherichia coli and Shigella spp. in water by using the polymerase chain reaction and gene probes for uid. *Appl. Environ. Microbiol.*, **57**(4): p. 1013-1017. (1991).
147. Chan, K.Y., *et al.*, Ultrasensitive detection of E. coli O157: H7 with biofunctional magnetic bead concentration via nanoporous membrane based electrochemical immunosensor. *Biosensors and bioelectronics*, **41**: p. 532-537. (2013).
148. Waswa, J., J. Irudayaraj, and C. DebRoy, *Direct detection of E. coli O157: H7 in selected food systems by a surface plasmon resonance biosensor*. *LWT-Food Science and Technology*, **40**(2): p. 187-192. (2007).
149. Wang, L., *et al.*, *A novel electrochemical biosensor based on dynamic polymerase-extending hybridization for E. coli O157: H7 DNA detection*. *Talanta*, **78**(3): p. 647-652. (2009).
150. Zhang, X., *et al.*, *Development of an electrochemical immunoassay for rapid detection of E. coli using anodic stripping voltammetry based on Cu@ Au nanoparticles as antibody labels*. *Biosensors and Bioelectronics*, **24**(7): p. 2155-2159. (2009).
151. Zhu, P., *et al.*, *Detection of water-borne E. coli O157 using the integrating waveguide biosensor*. *Biosensors and Bioelectronics*, **21**(4): p. 678-683. (2005).
152. Liao, J.C., *et al.*, *Development of an advanced electrochemical DNA biosensor for bacterial pathogen detection*. *The Journal of Molecular Diagnostics*, **9**(2): p. 158-168, (2007).
153. So, H.M., *et al.*, *Detection and Titer Estimation of Escherichia coli Using Aptamer-Functionalized Single-Walled Carbon-Nanotube Field-Effect Transistors*. *Small*, **4**(2): p. 197-201. (2008).
154. Roy, S. and Z. Gao, *Nanostructure-based electrical biosensors*. *Nano Today*, **4**(4): p. 318-334. (2009).
155. Shao, Y., *et al.*, *Graphene based electrochemical sensors and biosensors: a review*. *Electroanalysis: An International Journal Devoted to Fundamental and Practical Aspects of Electroanalysis*, **22**(10): p. 1027-1036. (2010).

156. Huang, Y., *et al.*, Graphene-based biosensors for detection of bacteria and their metabolic activities. *Journal of Materials Chemistry*, **21**(33): p. 12358-12362. (2011).
157. Cella, L.N., *et al.*, Nano aptasensor for protective antigen toxin of anthrax. *Analytical chemistry*, **82**(5): p. 2042-2047. (2010).